Third International Symposium on Precision Image-Guided Small Animal Radiotherapy Research

21-23 March 2016

Ghent, Belgium

Table of content

1. Introduction to the 3rd International Symposium on Precision Image-Guided Small Animal Radiotherapy Research

The organizers of the 3rd International Symposium on Small Animal Radiotherapy Research would like to welcome you to Ghent. This initiative grew from the realization that the new research field of precision image-guided small animal radiotherapy needs to bring together many disciplines to lead the field to fruition. A first very successful Symposium was held in Maastricht (Netherlands) in March 2013, followed by the second one in Vancouver in 2014.

The technological breakthroughs in animal imaging and precision irradiation have enabled experimental studies with research questions with a complexity which until recently could not be addressed. We can now, with unprecedented accuracy, proceed to discover radiation interaction mechanisms in whole organisms. New tumor models are emerging all the time. There is much hope to discover new synergistic effects of e.g. drugs or other agents, combined with radiotherapy. This new knowledge will help us in translating our findings towards human trials for combating several diseases, in particular cancer.

We brought together many of the leading specialists and vendors in the fields of radiobiology, radiotherapy, radiation physics, precision engineering, imaging, dose calculation, and others. We hope for a highly interactive two and a half day symposium with cutting edge science, stimulating discussions and debates, and we hope you may emerge from it with new ideas, new collaborations and an expanded research network.

Besides enjoying the Symposium, we hope that you will also have time to enjoy the beautiful historic city of Ghent, which is a hidden pearl.

We wish you an exciting Symposium!

Prof Christian Vanhove
Director Image and Signal Processing Group,
Ghent University-iMinds Medical IT department,
Ghent, Belgium

Prof Frank Verhaegen
Head of Clinical Physics Research
Maastro Clinic
Maastricht, the Netherlands

2. Symposium Organization

Scientific Organizers
Prof Christian Vanhove, University of Gent, Ghent, Belgium
(Christian.Vanhove@UGent.be)

Prof Frank Verhaegen, Maastro Clinic, Maastricht, the Netherlands
(frank.verhaegen@maastro.nl)

Logistic organizer
SmART Scientific Solutions B.V., Maastricht, the Netherlands
(frank.verhaegen@smartscientific.nl)

Symposium Secretariat
symposium@smartscientific.nl

Accessibility:
Please consult the following website for all travel information to the Symposium venue:

http://www.ugent.be/het-pand/en/accessibility

Internet access will be available throughout the conference:
Name wireless network: SmART 2016
Valid from 21–23/3/16
User name: guestSmart2
Password: h9OKuEe4

3. Sponsoring and endorsements

We would like to thank gratefully our generous sponsors:

GOLD: Precision X-ray Inc (USA)

SILVER: Xstrahl Life sciences (UK) and startup DoseVue NV

BRONZE: Faxitron, Advacam and startups Molecubes NV and SmART Scientific Solutions BV

The following organization is recommending the Symposium: The European Society for Radiotherapy and Oncology (ESTRO)

We also welcome the Institute of Physics (IOP)

4. Themed publication of Symposium papers in Br J Radiol

Br J Radiol is planning a **special feature on *Small Animal IGRT***, provisionally scheduled for early 2017, with *Guest Editors* ***Professor Frank Verhaegen*** and ***Professor Kevin Prise*** (BJR Editor-in-Chief (scientific)). The deadline for submitting papers for this issue is May 16 2016.

Instructions for authors can be found here: http://www.birpublications.org/page/ifa/bjr

More information may be obtained from: Laura.Harvey@bir.org.uk

---

New book on small animal imaging

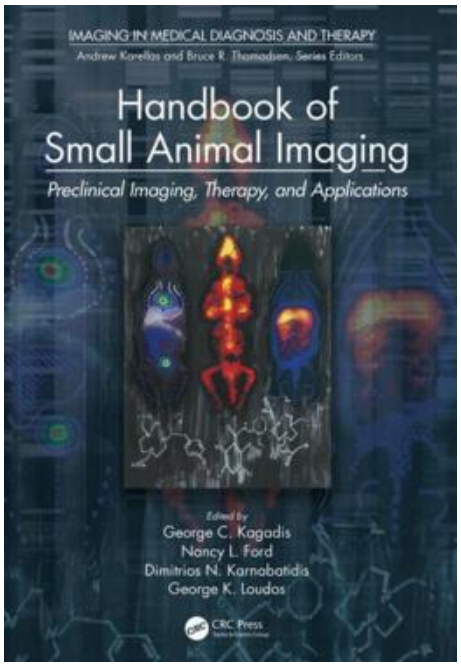

https://www.crcpress.com/Handbook-of-Small-Animal-Imaging-Preclinical-Imaging-Therapy-and-Applications/Kagadis-Ford-Karnabatidis-Loudos/9781466555686

5. Symposium program

Keynote Speaker

We're proud to open the Symposium with a seminar by one of the pioneers of small animal radiotherapy research, Professor Richard Hill from the University of Toronto. Professor Hill will give his seminar *"Tumour Response to Radiation Treatment"* on Monday March 21 in the first session.

Invited speakers

Tom Boterberg (Universiteit Gent)

Dirk de Ruysscher (Katholieke Universiteit Leuven, Maastro Clinic)

Matthias d'Huyvetter (Vrije Universiteit Brussel)

Mark Hill (University Oxford)

Bridget Koontz (Duke University)

Ala Yaromina (University Maastricht)

Symposium Short Program Overview

Sunday March 20
18.00-20.00: Registration desk open (Novotel hotel, Goudenleeuwplein 5, 9000 Gent)
Social event: Icebreaker reception Novotel

Symposium venue, 'Het Pand', Onderbergen 1, 9000 Gent
Monday March 21

8.00-9.00:	Registration
9.00-9.10:	Opening address
9.10-9.55:	Keynote address (prof R Hill)
9.55-10.40:	Tumor/normal tissue models
10.40-11.10:	Coffee break
11.10-12.10:	Research technology
12.10-12.30:	Discussion I
12.30-13.40:	Lunch
13.40-15.10:	Precision Radiotherapy
15.10-15.40:	Coffee break
15.40-17.15:	News from the manufacturers
17.15-17.35:	Discussion II

Free evening

Tuesday March 22

9.00-10.45:	Tumor/normal tissue models
10.45-11.15:	Coffee break
11.15-12.30:	Precision Radiotherapy
12.30-12.50:	Discussion III
12.50-14.00:	Lunch
14.00-15.30:	Imaging & Novel methods
15.30-16.00:	Coffee break
16.00-17.15:	Translational studies
17.15-17.35:	Discussion IV

18.30:	Boat to Dinner (canal close to Het pand)
19.00:	Dinner (St Pieters Abbey)

Wednesday March 23

9.00-10.00:	Dosimetry&Technology
10.00-10.30:	Coffee break
10.30-11.15:	Dosimetry&Technology
11.15-11.35:	Discussion V
11.35-11.45:	Best Young Speakers Awards & Closing the Symposium

Poster session
Throughout the Symposium all posters will be on display. There are no dedicated poster viewing times. Vendors will exhibit in the back of the meeting room.

Monday March 21

8.00-9.00	Registration
9.00-9.10	Opening address: C Vanhove, F Verhaegen (Ghent, Maastricht)
9.10-9.55	**KEYNOTE ADDRESS (Chair: C Vanhove)** R Hill - Tumour Response to Radiation Treatment
Tumor/normal tissue models. Chair: K Lauber	
9.55-10.10	C Cramer - Treatment planning and delivery of whole brain irradiation with hippocampal avoidance in rats
10.10-10.25	L Dubois - Nintedanib safely reduces radiation-induced lung damage in a mouse model of partial lung irradiation
10.25-10.40	J-L Ruan - Development of methods to study acute and late normal toxicity following pelvic radiotherapy using the small animal radiation research platform
10.40-11.10	**Coffee break**
Research technology. Chair: F Verhaegen	
11.10-11.40	INVITED: M Hill - Breathing gated irradiation using an image guided small animal irradiator: development and implementation
11.40-11.55	K Wang - A dual-use bioluminescence tomography guided system for small animal research platform (SARRP)
11.55-12.10	A-M Frelin - Study of respiratory gating in small animal radiotherapy
12.10-12.30	Discussion Session I- Moderators: C Vanhove, K Lauber
12.30-13.40	**Lunch**
Precision radiotherapy. Chair: B Koontz	
13.40-13.55	K Lauber - Fractionated radiotherapy in combination with anti-angiogenic therapy in an orthotopic, syngeneic glioma transplantation model
13.55-14.10	A Dietrich - Precise irradiation of orthotopic tumors using our non-commercial small animal image-guided radiotherapy platform (SAIGRT)
14.10-14.25	L Spiegelberg - Efficacy on tumor growth and safety towards normal tissues of the hypoxia activated prodrug TH-302 combined with targeted radiotherapy
14.25-14.40	M Dolera - Canine peripheral nerve sheath tumors: clinical aspects, MRI findings and comparison of palliation surgery and stereotactic radiotherapy
14.40-14.55	J Hartmann - Mice irradiation – setting, planning and dosimetry
14.55-15.10	S van Hoof - Automation of preclinical radiotherapy planning and the need for spatial degrees of freedom for irradiation
15.10-15.40	**Coffee break**
News from the manufacturers. Chair: R Weersink	
15.40-15.55	A Treverton (XStrahl)
15.55-16.10	P Dejean (PXi)
16.10-16.25	E d'Agostino (DoseVue)
16.25-16.40	R van Holen (Molecubes)
16.40-16.55	J Uher(Advacam)
16.55-17.10	S van Hoof (SmART Scientific Solutions)
17.10-17.30	Discussion Session II - Moderators: B Koontz, R Weersink
	Free evening

Tuesday March 22

Tumor/normal tissue models. Chair: D de Ruysscher	
9.00-9.30	INVITED: T Boterberg - The impact of neoadjuvant therapy on tumour microenvironment in colon cancer
9.30-9.45	A Henry - Role of osteopontin in glioblastoma radioresistance
9.45-10.00	J Odenthal - In vivo detection of invasive Head and Neck Squamous Cell Carcinoma by an anti-CD44v6 antibody
10.00-10.15	V Sosa Iglesias - Establishment of a relevant mouse orthotopic lung cancer model for testing alternative treatment strategies combined with image guided radiotherapy
10.15-10.30	P van Luijk - High-precision proton irradiation to study dose volume effects in rat tissues
10.30-10.45	T Hellevik - Tumorigenic effects of irradiated and non-irradiated cancer-associated fibroblasts co-transplanted with tumor cells in vivo
10.45-11.15	**Coffee break**
Precision radiotherapy. Chair: M Hill	
11.15-11.45	INVITED: A Yaromina - First preclinical studies in vivo evaluating therapeutic efficacy of radiation dose-painting: from conventional dose painting to “inverse dose painting”
11.45-12.00	K Butterworth - Comparison of CBCT imaging, dose calculation and biological response for high z nanoparticles
12.00-12.15	P Kazanzides - Treatment Planning Solutions for the Small Animal Radiation Research Platform (SARRP)
12.15-12.30	M Dolera - Frameless stereotactic radiotherapy alone and combined with temozolomide in canine gliomas
12.30-12.50	Discussion Session III – Moderators: D de Ruyscher, M Hill
12.50-14.00	**Lunch**
Imaging & Novel methods. Chair: L Dubois	
14.00-14.30	INVITED: M d’Huyvetter - Nanobody-Based Theranostics in Cancer
14.30-14.45	R Weersink - A Comparison of 3-D Bioluminescence Radiation Targeting using Analytical and Monte Carlo Models of Light Propagation
14.45-15.00	L Schyns - Optimizing dual energy CBCT protocols for preclinical imaging and radiation research
15.00-15.15	F Lallemand - Feasibility study of repetitive diffusion MRI after Neoadjuvant radiotherapy for following tumor microenvironment
15.15 – 15.30	E Brauer-Krisch - MRT (Microbeam Radiation Therapy (MRT): achievements and future perspectives
15.30-16.00	Coffee break
Translational studies. Chair: R Hill	
16.00-16.30	INVITED: B Koontz - Bedside to Bench in Normal Tissue Radiobiology: translating patient experience into animal models
16.30-16.45	O De Wever - Radiation-induced lung damage promotes breast cancer lung-metastasis: use of SARRP in an orthotopic mouse model of breast cancer
16.45–17.15	INVITED: D de Ruysscher - Transforming mice to mini-humans: A valid strategy for translational research?
17.15-17.35	Discussion Session IV - Moderators: L Dubois, R Hill
18.30	**Boat to Symposium Dinner (canal close to Het pand)**
19.00	**Symposium Dinner (St Pieters Abbey)**

Wednesday March 23

Dosimetry&Technology. Chair: P Kazanzides	
9.00-9.15	J Stewart - Spatial frequency dosimetric performance limitations for dose optimization in preclinical investigations
9.15-9.30	B van der Heyden - The impact of breathing motion on a mouse lung tumor irradiation using the 4D MOBY phantom
9.30-9.45	C Eccles - Intra- and inter- fraction variation in animal position for multi-fraction lung radiation on a small animal radiation research platform
9.45-10.00	M Reinhart - Development of a novel analytical dose calculation software for animal radiotherapy
10.00-10.30	**Coffee break**
Dosimetry&Technology. Chair: K Butterworth	
10.30-10.45	C Le Deroff- Plastic scintillating optical fiber dosimetry for small animal irradiation
10.45-11.00	M Ghita - Biologically optimized commissioning study for small animal irradiation platform
11.00-11.15	F Verhaegen - ESTRO Work group on Technology for Precision Small Animal Radiotherapy Research
11.15-11.35	Discussion session V – Moderator: P Kazanzides, K Butterworth
11.35-11.45	C Vanhove, F Verhaegen – Best Young Speaker Awards & closing the Symposium

Abstracts
Oral presentations

Tumour Response to Radiation Treatment

RP Hill

Ontario Cancer Institute, Toronto, Canada
Campbell Family Institute for Cancer Research
Departments of Medical Biophysics and Radiation Oncology, University of Toronto, Toronto, Canada

Understanding the background of tumour response to irradiation informs methods to test the potential efficacy of new combination treatments. Early studies of the radiation response of tumour cells focused on the inhibition of long-term proliferative potential (defined as survival) as this was regarded as the critical element of tumour (re)growth. Despite the focus on cellular response the well recognized four 'Rs' of radiotherapy (repair, redistribution, reoxygenation and repopulation) did not include intrinsic radiosensitivity (the 5th 'R') until fairly recently. This was consistent with a general belief that, apart from hematological malignancies, the differing intrinsic radiosensitivities of cancer cells (usually defined by the slope of the survival curve) were relatively small (other than that caused by hypoxia) compared with differences that can occur with chemotherapeutic drugs. More recently this has been questioned and, for example, reducing DNA repair capacity either by drugs, or genetically, has illustrated that major modifications of cellular radiosensitivity are possible, although it remains a concern that for therapy purposes such modifications need to be specific for the tumour cell population. That cells can often undergo a few divisions following irradiation before dying is the basis of the use of clonogenic assays to assess the radiosensitivity of cells in vitro and in vivo and is the reason that short term functional assays are of limited value. This effect also plays an important role in tumour response in vivo, since it means that the early regression of tumours following irradiation does not necessarily reflect the number of cells for which long-term proliferative potential had been effectively inactivated. The development of tumor growth delay as a measure of treatment efficacy recognized this concern, since it requires regrowth of the tumour to a size at least as large as the pretreatment size. Even this approach however, does not necessarily address the response of the most resistant (cancer stem) cells that may be responsible for tumour regrowth. These can only be addressed using tumour control assays. In this presentation I will discuss various aspects of tumour response and discuss some approaches using a small animal irradiator to examine issues related to the tumour microenvironment that is increasingly recognized as an important component of tumour response to irradiation.

Treatment planning and delivery of whole brain irradiation with hippocampal avoidance in rats

CK Cramer[1], SW Yoon[1], M Reinsvold[1], KM Joo[1,4], D Miles[1], H Norris[1], RC Hood[1], JD Adamson[1], RC Klein[2,5], DG Kirsch[1,3*], M Oldham[1*]

[1] Department of Radiation Oncology, Duke University Medical Center
[2] Department of Psychiatry, Durham VA
[3] Department of Pharmacology & Cancer Biology, Duke University Medical Center
[4] Department of Anatomy and Cell Biology, Sungkyunkwan University School of Medicine
[5] Department of Psychiatry and Behavioral Sciences, Duke University Medical Center
*Co-senior authors

Background: Despite the clinical benefit of whole brain radiotherapy (WBRT), patients and physicians are concerned by the long-term impact on cognitive functioning. Many studies investigating the molecular and cellular impact of WBRT have used rodent models. However, there has not been a rodent protocol comparable to the recently reported Radiation Therapy Oncology Group (RTOG) protocol for WBRT with hippocampal avoidance (HA) which is intended to spare cognitive function. The aim of this study was to develop a hippocampal-sparing WBRT protocol in Wistar rats. Methods: The technical and clinical challenges encountered in hippocampal sparing during rat WBRT are substantial. Three key challenges were identified: hippocampal localization, treatment planning, and treatment localization. Hippocampal localization was achieved with sophisticated imaging techniques requiring deformable registration of a rat MRI atlas with a high resolution MRI followed by fusion via rigid registration to a CBCT. Treatment planning employed a Monte Carlo dose calculation in SmART- Plan and creation of 0.5cm thick lead blocks custom-shaped to match DRR projections. Treatment localization necessitated the on-board image-guidance capability of the XRAD C225Cx micro- CT/micro-irradiator (Precision X-Ray). Treatment was accomplished with opposed lateral fields with 225 KVp X-rays at a current of 13mA filtered through 0.3mm of copper using a 40x40mm square collimator and the lead blocks. A single fraction of 4Gy was delivered (2Gy per field) with a 41 second beam on time per field at a dose rate of 304.5 cGy/min. Dosimetric verification of hippocampal sparing was performed using radiochromic film. In vivo verification of HA was performed after delivery of a single 4Gy fraction either with or without HA using γ-H2Ax staining of tissue sections from the brain to quantify the amount of DNA damage in rats treated with HA, WBRT, or sham- irradiated (negative controls).

Results: The mean dose delivered to radiochromic film beneath the hippocampal block was 0.52Gy compared to 3.93Gy without the block, indicating an 87% reduction in the dose delivered to the hippocampus. This difference was consistent with doses predicted by Monte Carlo dose calculation. The Dose Volume Histogram (DVH) generated via Monte Carlo simulation showed an underdose of the target volume (brain minus hippocampus) with 50% of the target volume receiving 100% of the prescription isodose as a result of the lateral blocking techniques sparing some midline thalamic and subcortical tissue. Staining of brain sections with anti- phospho-Histone H2A.X (reflecting double-strand DNA breaks) demonstrated that this treatment protocol limited radiation dose to the hippocampus in vivo. The mean signal intensity from γ-H2Ax staining in the cortex was not significantly different from the signal intensity in the cortex of rats treated with WBRT (5.40 v. 5.75, P= 0.32). In contrast, the signal intensity in the hippocampus of rats treated with HA was significantly lower than rats treated with WBRT (4.55 v. 6.93, P= 0.012). Conclusion: Despite the challenges of planning conformal treatments for small volumes in rodents, our dosimetric and in vivo data show that WBRT with HA is feasible in rats. This study provides a useful platform for further application and refinement of the technique.

Nintedanib safely reduces radiation-induced lung damage in a mouse model of partial lung irradiation

D De Ruysscher[1,2], P Granton[1], N G Lieuwes[1], S van Hoof[1], L Wollin[3], F Verhaegen[1], L Dubois[1]

[1]Department of Radiation Oncology (MAASTRO), GROW – School for Oncology and Developmental Biology, Maastricht University Medical Center, The Netherlands
[2]KU Leuven - University of Leuven, University Hospitals Leuven, Department of Radiation Oncology, B-3000 Leuven, Belgium
[3]Boehringer Ingelheim Pharma GmbH & Co. KG, Biberach, Germany

Introduction: The indolinone small-molecule derivative nintedanib has been originally designed as an anti-angiogenic receptor tyrosine kinase inhibitor targeting VEGFR, FGFR and PDGFR for the treatment of cancer by occupying the intracellular ATP-binding site of the specific tyrosine kinases. Additionally, preclinically nintedanib has demonstrated potent anti-fibrotic and anti-inflammatory activity. Nintedanib was recently approved in the US and EU for the treatment of idiopathic pulmonary fibrosis (IPF). The aim of this study was to assess the efficacy and safety of nintedanib in a mouse model of partial lung irradiation using a precision image-guided small animal irradiator.

Materials & Methods: 266 C57BL/6 adult male mice were irradiated with a single fraction radiation dose of 0, 4, 8, 12, 16 or 20 Gy using 5-mm circular parallel-opposed fields targeting the upper right lung with a precision image-guided small animal irradiator (PXRAD225Cx, PXI Inc, USA) sparing heart and spine based on micro-CT images acquired at 200 µm resolution. One week post irradiation, mice were randomized across nintedanib daily oral gavage treatment with 0, 30 or 60 mg/kg respectively for a total of 39 weeks. Micro-CT imaging was repeated on a monthly basis. At the end of the experiment, lungs were removed and processed for H&E, Van Gieson's and Masson's trichrome staining to evaluate the fibrotic phenotype, scoring alveolar wall thickness, edema, fibrosis, inflammation, macrophage infiltration, atelectasis and vasculitis.

Results: CT images indicated increased lung density in the late stage imaging time points of irradiated mice after 20 Gy which was spatially limited to the irradiated part of the lung. This increased density was consistent with the development of fibrosis, confirmed by an increased fibrotic phenotype scored by an increase in alveolar wall thickness, interstitial edema, interstitial and perivascular fibrosis, perivascular inflammation, interstitial and alveolar macrophages, atelectasis and vasculitis. Although macroscopically, no decrease in CT density could be observed, nintedanib was able to reduce the microscopic fibrotic phenotype, in particular interstitial edema, interstitial and perivascular fibrosis, perivascular inflammation and vasculitis, without adverse effects.

Conclusion: Nintedanib efficiently and safely reduces radiation-induced lung fibrosis after partial lung irradiation in mice. Since, as expected, nintedanib did not affect alveolar wall thickness and macrophage involvement, no significant changes in lung density could be observed by CT imaging. Based on its protective effect, nintedanib might be safely introduced in clinical trials for patients treated with irradiation to the lungs.

Development of methods to study acute and late normal toxicity following pelvic radiotherapy using the small animal radiation research platform

[1]J-L Ruan, [1]B Groselj, [1, 2]H Scott, [1]J Thompson, [3]C Scudamore, [1]AE Kiltie

[1]CRUK/MRC Oxford Institute for Radiation Oncology, University of Oxford, UK
[2]Nuffield Department of Surgical Sciences, University of Oxford, UK
[3]Mary Lyons Centre MRC Harwell, UK

Introduction: The development of small animal radiation research platforms (SARRP) with attached cone-beam CT scanners has allowed us to irradiate mice with protocols similar to those used in human patients. We are interested in the treatment of bladder cancer with radiotherapy and chemoradiation. In humans, chemoradiation causes more severe bladder and bowel toxicity than radiation alone, so there is an urgent clinical need to find less morbid treatments. Using our SARRP, we have developed methods to assess acute and late normal tissue toxicities in mice following treatment to the bladder and surrounding intestines.

Materials&Methods: For acute normal tissue toxicity assessment, female CD1 nude mice were treated supine with a single dose of 10, 12, or 14 Gy (n=2 per group) to the lower abdomen in an Xstrahl SARRP using a 220 kV 356 degree arc treatment with a 12 mm circular collimator. Mice were culled at 3.75 days and intestinal Swiss Rolls made for use in a modified crypt assay. For late normal tissue toxicity assessment, mice were treated vertically to remove small intestine from the irradiation field, head down in the SARRP to a dose of 25 Gy in five daily fractions, using a 356 degree arc and 10 mm collimator, centred on the posterior caudal edge of the bladder wall. At 11 weeks post treatment, faeces were collected from individual mice for 24 hours and pellets weighed and measured. Mice were culled at 12 weeks and formalin-fixed, paraffin-embedded bladder and intestines examined histopathologically by a veterinary pathologist.

Results: In the crypt assay, there was a 49.6%, 82.9% and 86.6% crypt loss after 10, 12 and 14 Gy respectively. In mice assessed for late toxicity there was a maximal median weight loss of 1.6% (range (+)1.8-4%) which returned to baseline 6 days post-treatment. There was no significant difference in mean weight of dried faeces or mean number of faecal pellets, and over 85% of pellets were >4.5 mm in length in both irradiated (n=3) and unirradiated (n=5) groups. On histopathological assessment, one of the irradiated mice had mild large intestinal inflammation and crypt hyperplasia.

Conclusion: Using our small animal radiation research platform, we have developed a method to assess acute and late bowel toxicity in mice, applicable to the treatment of bladder, gynaecological and bowel malignancies. The method also permits assessment of potential increased toxicities due to the addition of radiosensitising agents in chemoradiation schedules.

Breathing gated irradiation using an image guided small animal irradiator: development and implementation

MA Hill, J Thompson, A Kavanagh, IDC Tullis, RG Newman, J Beech, D Allen, A Gomes, P Kinchesh, S Gilchrist, V Kersemans, S Smart, E Fokas, B Vojnovic

CRUK/MRC Oxford Institute for Radiation Oncology, Gray Laboratories, Department of Oncology, University of Oxford, ORCRB Roosevelt Drive, Oxford OX3 7DQ, UK

Introduction: The development of image-guided small animal irradiators represents a significant improvement over standard animal irradiation systems enabling preclinical treatments to mimic radiotherapy in humans. The ability to deliver tightly collimated targeted beams in conjunction with gantry or couch rotation, has the potential to maximise tumour dose while sparing normal tissues. Although cone beam CT (CBCT) is intended to enable accurate targeting, its inherent low degree of soft tissue contrast does not enable identification of the abdominal organs. Furthermore, current commercial platforms do not incorporate respiratory gating as required for accurate and precise targeting in organs subject to breath-related motions.

Materials & Methods: To address these issues, co-registration with MRI images has been implemented to allow the identification of sites not resolved using CBCT. Importantly, a new treatment head assembly for the Xstrahl Small Animal Radiation Research Platform (SARRP) has been designed at Oxford. This includes an integrated transmission ionisation chamber to monitor beam delivery, a targeting laser exiting the centre of the beam collimator, a motorised beam hardening filter assembly that allows for automated changing of filters and a fast x-ray shutter subsystem. The incorporated X-ray shutter not only reduces timing errors but also allows beam gating during imaging and treatment, with irradiation only taking place during the breathing cycle when tissue movement is minimal. The breathing cycle is monitored with a modulated near infrared (850 nm) light emitting diode source, its light being delivered with a polymer optical fibre and illuminating the animal's body. Diffuse reflectance from the moving surface is picked up by an adjacent fibre and the resulting signal is processed by a synchronous detector/lock-in amplifier. Following thresholding of the resulting signal, delays are added around the inhalation phase, gating it out and enabling the 'no movement' period to be isolated: this is used to close the x-ray shutter. Using this system, irradiation can either be performed for a predetermined time of x-ray exposure, or through measurement and integration of current from the transmission monitor ionisation (corrected locally for temperature and atmospheric pressure variations).

Results: Successful registration was achieved between MRI and CBCT images with minimal movement of internal organs observed following multiple movements between imaging devices. The ability to successfully deliver breathing gated x-ray irradiations has been demonstrated by comparing movies obtained using planar x-ray imaging with and without breathing gating, in addition to comparing the dose profile observed from a collimated beam on EBT3 radiochromic film mounted on the animals' chest.

Conclusion: The development of techniques for co-registration of MRI and CBCT images enables the identification and targeting of sites not previously visible using CBCT alone. Altogether, the development of breathing gated irradiation using the new treatment head facilitates improved dose delivery even during animal movement and constitutes an important new tool for preclinical radiotherapy studies that is particularly well suited for treatments of orthotopic tumours or other organs that are not readily identified.

A dual-use bioluminescence tomography guided system for small animal research platform (SARRP)

K K-H Wang (1), B Zhang (1), P T Tran (1, 2), I Iordachita (3), M S Patterson (4), J W Wong (1)

Affiliations: (1). Department of Radiation Oncology and Molecular Radiation Sciences, Johns Hopkins University, MD, USA, (2). Departments of Oncology and Urology, Johns Hopkins University, MD, USA, (3). Laboratory for Computational Sensing and Robotics, Johns Hopkins University, MD, USA, (4). Department of Medical Physics and Applied Radiation Sciences, McMaster University, ON, Canada

Introduction: We developed a novel dual-use configuration for an integrated x-ray cone beam CT (CBCT) and bioluminescence tomography (BLT) imaging system with the SARRP that can function as a standalone system for longitudinal imaging research and on-board the SARRP to guide irradiation. BLT is expected to provide 3D radiation guidance for low contrast soft tissue target and reveal the cell viability.

Materials & Methods: The optical assembly includes a CCD camera, lens, filter wheel, 3-way mirrors, and a light-tight enclosure. The rotating mirror system directs the optical signal from the animal surface to the camera at multiple projections over 180 degree. Multiple filters are used for multispectral imaging to enhance localization accuracy using BLT. SARRP CBCT provides anatomical information and geometric mesh for BLT reconstruction. To facilitate dual use, the 3-way mirror system is cantilevered in front of the camera. The entire optical assembly is driven by a 1D linear stage to dock onto an independent mouse support bed for standalone application or on-board SARRP to provide radiation guidance. After completion of on-board optical imaging, the system is retracted from the SARRP to allow irradiation of the mouse with full radiation shielding.

Results: A tissue-simulating phantom and a mouse model with a luminescence light source are used to demonstrate the function of the dual-use optical system. Feasibility data have been obtained based on a manual-docking prototype. The center of mass of light source determined with on-board BLT is within 1±0.2 mm of that with CBCT. The performance of the motorized system is expected to be the same and will be presented.

Conclusion: We anticipate the motorized dual use system provide significant efficiency gain and positioning error reduction over our manual docking system and off-line system. By also supporting off-line longitudinal studies independent of the SARRP, the dual-use system is a highly efficient and cost-effective platform to facilitate optical imaging for pre-clinical radiation research.

Study of respiratory gating in small animal radiotherapy

A-M Frelin-Labalme (1,2), V Beaudouin (3)

(1) Grand Accélérateur National d'Ions Lourds (GANIL), CEA/DSM-CNRS/IN2P3, Boulevard Henri Becquerel, 14076 Caen, France
(2) Archade, Centre François Baclesse, 3 Avenue du Général Harris, 14076 Caen, France
(3) Cyceron, CEA/DSV/I2BM/SHFJ/LDMTEP, Campus Jules Horowitz, Bd Henri Becquerel, 14076 Caen, France

Introduction: Major progress has been done in small animal radiotherapy with the development of precision irradiators. They allow preclinical irradiations much more similar to complex radiotherapy treatments. Yet some applications, such as mobile tumor irradiations, have not reached the same level of accuracy in preclinical irradiation as in modern radiotherapy. Two approaches are currently available for small animal mobile tumor irradiation: either extending the irradiation field according to tumor motion during the respiratory cycle (increasing the dose to healthy tissues), or treating during breath-holdings of the animal (increasing invasiveness). In this work we investigated a new alternative which is gated irradiation of free-breathing animals.

Materials&Methods: Gated irradiation was here tested on a dedicated phantom, developed in our laboratory, suited to CBCT and TEP imaging and producing various 1D motions. Its performances were evaluated with sinusoidal and exponential movements of variable amplitudes and frequencies. These motions were imaged with a Siemens Inveon preclinical micro PET/CT, and the X-Rad 225Cx irradiator (PXI) installed in Caen in the frame of Archade (Rec-Hadron project).

In a second time, gated irradiation was investigated by irradiating our phantom with a 15mm diameter vertical beam. A gafchromic EBT3 film was placed on top of the phantom for each measurement. First, the phantom was irradiated immobile to determine the nominal dose distribution of the beam. Secondly, a sinusoidal motion (1Hz, ~5mm amplitude) was applied to the phantom which was irradiated without gating. Finally, a gated irradiation, controlled by the phantom position, was performed with the same motion. Three gate widths of 550, 430 and 300ns were tested.

Results: Our phantom was able to produce various motions of amplitudes ranging from 0.3mm to 10.4mm, and frequencies from 0.5Hz to 2Hz, thus representative to mice and rats respiratory movements. The evaluation of sinusoidal motion has shown frequency stability better than 0.05% regardless of the amplitude and frequency applied. It has also shown that mechanical clearance and motor power reduction caused a slight damping at the beginning and the end of the translation when small amplitudes were applied. Nevertheless, discrepancies between experimental amplitude and sinusoidal fit stayed below 0.45mm. Exponential motions have also been successfully tested to simulate more realistic motions.

The second part of this study has shown that gated irradiation could efficiently compensate the sinusoidal motion of the phantom. Indeed, without gated irradiation the dose distribution width (measured at 10% of Dmax) was of 20.2mm instead of 15mm when the phantom is immobile. Gated irradiation allowed reducing this width to 18.2mm, 15.7mm and 15.2mm respectively for gate width of 550, 430 and 300ns. The 430nm gate appeared to be a good compromise because it provided a dose distribution very close to the nominal one while limiting the irradiation time increase.

Conclusion: This study has shown the feasibility of gated irradiation with precision irradiators, providing a new alternative to breath-holding in preclinical irradiation of mobile tumors. The evaluation of smaller collimators is under progress and in-vivo validation is intended.

Fractionated radiotherapy in combination with anti-angiogenic therapy in an orthotopic, syngeneic glioma transplantation model

V Albrecht (1), J Schuster (1), M Proescholdt (2), D Piehlmaier (3), K Unger (3), C Belka (1), M Niyazi (1), K Lauber (1)

Affiliations: (1) Clinic for radiotherapy and radiation oncology, LMU Munich; (2) Department of Neurosurgery, University Hospital Regensburg, (3) Research Unit of Radiation Cytogenetics, Helmholtz Center Munich, Neuherberg, Germany

Introduction: Glioblastoma (GBM) is the most common primary brain tumor in adults. Despite intense treatment, including surgery and radiochemotherapy, prognosis is dismal with a median overall survival time of only 15 months. The vascular endothelial growth factor-A (VEGF-A) has been identified as one of the key regulators of neoangiogenesis in these highly vascularized tumors. Therefore, disruption of the VEGF-A signaling cascade by neutralizing VEGF-A and preventing ligation of its receptors appeared to be a promising approach for targeting neoangiogenesis. However, in recent phase III trials application of the VEGF-A blocking antibody bevacizumab in combination with radiochemotherapy failed to prolong overall survival in newly diagnosed GBM despite increasing progression-free survival and improving performance status. The aim of our study was to analyze the treatment effects of radiotherapy in combination with bevacizumab in a clinically relevant setting. Therefore, we established an orthotopic, syngeneic mouse glioblastoma model and subjected it to fractionated radiotherapy in combination with the bevacizumab mouse analogue G6-31.

Materials & Methods: GL261 mouse GBM cells were stereotactically transplanted into the frontal lobe of C57/BL6 mice and tumors were allowed to grow for one week. Radiation therapy was performed with a Small Animal Radiation Research Platform (SARRP, Xstrahl) which incorporates contrast agent-CT (CA-CT)-based imaging followed by high precision radiation delivery. Fractionated irradiation with daily doses of 2 Gy up to a cumulative dose of 20 Gy was administered with or without accompanying VEGF-A blockade by the mouse bevacizumab analogue G6-31. Overall survival and tumor size were monitored, and histological analyses are currently being performed.

Results: Stereotactic implantation of GBM was successfully accomplished, fractionated irradiation was implemented by CA-CT-based image guidance, and tumor growth was successfully monitored by serial CA-CT scans. The single agent treatments led to a significant delay in tumor growth and prolongation of survival as compared to the sham-treated controls. Importantly, the strongest therapeutic effects were observed with the combined treatment. Histological details, including vessel density and structure, as well as markers of cell death induction, and transcriptomic profiling of tumor and normal tissue are currently under investigation.

Conclusions: This pilot study shows that syngeneic, orthotopic glioblastoma transplants combined with stereotactically delivered radiotherapy are feasible and clinically relevant in vivo models for evaluating the therapeutic efficacy of multimodal treatment approaches based on fractionated irradiation.

Precise irradiation of orthotopic tumors using our non-commercial small animal image-guided radiotherapy platform (SAIGRT)

A Dietrich[1,2], A Fursov[1,2], F Tillner[2,3], S Löck[2], R Haase[2,4], Ml Baumann[1,2,3,5], M Krause[1,2,3,5], R Bütof[2,3]

[1]German Cancer Consortium (DKTK), Dresden, Germany, German Cancer Research Center (DKFZ), Heidelberg, [2]OncoRay – National Center for Radiation Research in Oncology, Medical Faculty and University Hospital Carl Gustav Carus, Technische Universität Dresden, [3]Department of Radiation Oncology, University Hospital Carl Gustav Carus, Technische Universität Dresden, [4]Scientific Computing Facility, Max Planck Institute for Molecular Cell Biology and Genetics, Dresden
[5]Helmholtz-Zentrum Dresden – Rossendorf, Institute of Radiooncology

Introduction: We envision performing translational radiooncology with comprehensive imitation of the clinical practice. Therefore, we developed the Small Animal Image-Guided Radiotherapy (SAIGRT) platform, which allows for precise and accurate isocentric conformal irradiation of small animals using 360° gantry rotation and X-ray imaging such as fluoroscopy and cone beam CT (CBCT). To enable irradiation of orthotopic glioblastoma models in mice, contrast-enhanced imaging protocols were implemented and evaluated. Accurate beam positioning was verified by fluoroscopy and histological staining.

Methods and Results: U87MG glioblastoma cells (3×10^5 cells in 3 µl) were transplanted intracranially using a stereotactic frame. Tumor growth was assessed weekly via contrast-enhanced MRI (nanoScan® PM PET/MRI, Mediso) using 150 µl Omniscan™ 50 (i.p. 10 min prior to imaging). For tumor localization, a contrast-enhanced CBCT protocol was established using i.v. injection of 150 µl Ultravist 370 directly before imaging. Thereby, the irradiation workflow could be adapted from our lung tumor model. Precise beam application was validated by both, radiographic position verification through the secondary collimator prior to irradiation and staining of DNA double strand breaks via γH2AX on fixed tumor tissue. However, the comparison of respective CBCT and MRI slices revealed an overestimation of the tumor dimension during treatment planning which was caused by the weak contrast-enhancement in the CBCT images.

Conclusion: An orthotopic glioblastoma model was successfully used to adapt the already established irradiation workflow to this entity. The contrast-enhancement of CBCT imaging using an iodine-based contrast agent was weak but feasible for target definition in the U87MG model. However, the demarcated and non-invasive growth of U87MG is untypical for glioblastoma. This may favour the tumor-to-background contrast and other glioblastoma models, which better mirror the clinical situation, may be much more difficult to delineate. Thus, multi-modality imaging using MRI and CBCT in combination for treatment planning is mandatory and currently implemented. Eventually, this would further approximate the experimental protocol to the clinical standard for glioblastoma patients. The histological beam visualization via DNA damage staining is feasible to evaluate dose distribution patterns of different radiation types (e.g. photons, protons). The flexibility of the SAIGRT system provides the basis for comparative radiobiological studies in this context. The SAIGRT system enables the integration of additional equipment (e.g. computerized collimation or supplemental imaging modalities). This flexibility in combination with its non-commercial character facilitates the distribution to additional partner sites, which has been recently realized within the German cancer consortium (DKTK). This will allow for multicenter preclinical studies using the same hard- and software basis with the potential to adapt the SAIGRT system to the respective on-site expertise.

Efficacy on tumor growth and safety towards normal tissues of the hypoxia activated prodrug TH-302 combined with targeted radiotherapy

L Spiegelberg (1), SJ van Hoof (1), NG Lieuwes (1), R Biemans (1), A Yaromina (1), M Berbee (1), P Lambin (1), F Verhaegen (1), L Dubois (1)

(1) Department of Radiation Oncology (MAASTRO), GROW – School for Oncology and Developmental Biology, Maastricht University Medical Centre, Maastricht, the Netherlands

Tumor hypoxia is a well-known phenomenon that is present in most solid tumors and causes resistance to conventional anti-cancer therapies. The severe hypoxia present in tumors is unique and regulates tumor prognosis and therefore forms an attractive target. Indeed, several generations of hypoxia-activated prodrugs (HAPs) have been developed. These agents are reduced in the absence of oxygen and fragment into cytotoxins that kill the hypoxic cells. The currently most studied and advanced HAP, preclinically as well as clinically, is TH-302. It has been shown in different preclinical tumor models to delay tumor growth and improve survival. In clinical phase I and II studies, MTDs have been defined and tumor response seems favorable. Phase III studies are currently underway.

However, these studies regard TH-302 monotherapy or the combination of TH-302 with chemotherapy, while the combination with radiotherapy has not been extensively investigated. We aim to study the effect of this combination in preclinical models, regarding both tumor growth and normal tissue toxicity. Previously, we showed an enhancement of therapeutic outcome of the combination of TH-302 with RT in preclinical models of H460 NSCLC and Rhabdomyosarcoma R1. Our next goal is to confirm these results in models of esophageal cancer, a disease of which the incidence is increasing and that is rarely curable. Most esophageal cancers have hypoxic areas, making them susceptible for TH-302 therapy.

Along with this, normal tissue toxicity due to the combination or TH-302 and radiotherapy, needs to be assessed. In mono- and chemotherapy-combination studies, dose limiting toxicities consisted of skin and mucosal reaction. The combination of TH-302 with doxorubicin increased the hematologic toxicity of doxorubicin. In order to investigate whether TH-302 has an effect on radiation-induced toxicities, we use both short- and long term radiation-induced toxicity models. For the short term, we irradiate the gut of TH-302 treated mice with a single dose of 10 Gy. Three-and-a-half days after RT, mice are sacrificed and crypt colony- and mucosal surface assays are performed. In addition citrullin levels will be determined. For long term toxicity, TH-302 treated mice are irradiated with a 20 Gy single dose using targeted SmART irradiation directed at 25% of the right lung volume based on baseline CT imaging using SmART-plan treatment planning software. Subsequent CT scans will be made at different time-points for up to 12 months post-RT, when mice will be sacrificed and lung tissue will be histologically investigated for fibrosis. The first results regarding both the esophageal cancer model and the normal tissue toxicity studies will be presented at the symposium.

Canine peripheral nerve sheath tumors: clinical aspects, mri findings and comparision of palliation surgery and stereotactic radiotherapy

M Dolera L Malfassi, S Marcarini, S Paves, G Mazza, M Sala, N Carrara, S Finesso, G Urso

La Cittadina Fondazione Studi e Ricerche Veterinarie, Romanengo - CR, Italy

Introduction: No updates for canine peripheral nerve sheaths tumor (PNST) appeared in recent literature. The aim of this study was to evaluate the correlation between clinical aspects and MRI findings of tumors involving a major peripheral nerve, plexus or root and to determine the survival time in dogs treated with palliation, surgery or stereotactic radiotherapy (SRT).

Materials & Methods: Records of dogs with PNST evaluated from 2000 to 2014 were reviewed to determine signalment, duration of clinical signs, neurological examination, MRI features, treatment option (palliation, surgery, stereotactic hypo fractionated radiotherapy). Time to first event, survival times and statistical differences across categories were calculated by the Kaplan-Meier product limit method and log-rank test.

Results: Forty-seven dogs (median age 9 years, male:female ratio 1.76) were included, with Labrador retriever over represented (17%). Roots lesions were the most frequent (46.8%), with C5-T1, V nerve and left side more involved (25.5%, 19.1% and 61.7%). Presenting sings were lameness, paresis and pain. Mean duration of clinical signs was 90 days. MRI findings comprises increased diameter, hyper intense and contrast enhancing nerve roots (57.1%), plexus or peripheral nerve (42.9%), focal hypomiotropy and muscle hyper intensity (73%). The time to first event was 30 days after surgery and 240 days after SRT. Overall mean survival was 97, 144 and 371 days with palliation, surgery and SRT.

Conclusion: A predilection for Labrador retriever is observed. Comparing our results with published data, SRT seem to promise better results than palliation or surgery and warrant further evaluation.

Mice irradiation – setting, planning and dosimetry

J Hartmann(1), J Wölfelschneider(1), A Hölsken(2), U Gaipl(1), C Bert(1), B Frey(1)

(1) University Hospital Erlangen and Friedrich-Alexander-Universität Erlangen-Nürnberg, Department of Radiation Oncology, Universitätsstraße 27, 91054 Erlangen, Germany
(2) University Hospital Erlangen, Institute of Neuropathology, Schwabachanlage 6, 91054 Erlangen, Germany

Introduction: Special small animal irradiation systems were developed in the last years, but still simpler irradiation systems are applied due to simplicity and running costs. This study defines a clinical standard protocol for small animal partial body irradiation using a clinical linear accelerator usually performed for stereotactic treatments that provide the possibility for tumor conformal mice irradiation. Further dosimetrical verifaction for small field sizes are introduced and quantified.

Materials & Methods: Brain tumors in mice were irradiated separately while sparing of healthy tissue. For that reason, computed tomography and magnetic resonace imaging were applied to perform a segmentation of target volume and organs at risk. Afterwards, three 6 MV photon beams with gantry angles of 90°, 0° and 270° were planned for a total dose of 18 Gy applied in 10 fractions. Each mouse was positioned insided a self-made applicator and the mouse position were daily verified by the clinical ExacTrac system before irradiation. Different dosimetric methods, as ionization chamber and film measurements were applied for dose verification.

Results: All mice tolerated the irradiation with the total prescribed dose in the tumor volume. The self-made applicator was suitable for individual positioning and irradiation of mice during anaesthesia. Positioning with the ExacTrac system was possible with a sub-millimeter accuracy. Further, a single mouse could be treated in less than ten minutes including positioning and irradiation.

Conclusion: The defined treatment protocol for small animal partial body irradiation with a common clinical treatment planning system, the positioning with the ExacTrac system, the clinical linear accelerator and the used fractionation scheme was feasible to apply. The brain tumor in mice could be irradiated individually while sparing of healthy tissue. Dosimetrical verification of the treatment plan was performed succesfully.

Automation of preclinical radiotherapy planning and the need for spatial degrees of freedom for irradiation

SJ van Hoof (1), J Verde (1), LEJR Schyns (1), B van der Heyden (1), F Verhaegen (1)

(1) Department of Radiation Oncology (MAASTRO), GROW School for Oncology and Developmental Biology, Maastricht University Medical Center, the Netherlands

Introduction: Hardware for precision image-guided small animal radiotherapy is evolving rapidly and catching up with clinical irradiation capabilities. These improvements of preclinical radiotherapy research platforms require equally improving software and algorithms to plan, evaluate and control the hardware. However, since treatment goals and restrictions in preclinical research can be vastly different from the clinical setting, it is not necessarily the case that preclinical research platforms require or need to pursue the same development path their clinical counterparts have gone through. The purpose of this study is to improve treatment planning automation and employ it to evaluate the need for degrees of freedom in beam positioning.

Materials & Methods: For small animal treatment planning we used a research version of the Monte Carlo based treatment planning system SmART-Plan. SmART-Plan was extended with a module for beam-on time optimization. This optimizer determines Pareto-optimal solutions using user-provided constraints and weights for objectives. SmART-Plan was also extended to enable the processing the dose distributions of a large numbers of radiation beams, to subsequently use those data as input for the optimization algorithms. Further extension was performed with Matlab-based software to generate beam configurations to mimic dose painting. Treatment plans were delivered using the preclinical radiotherapy platform Precision X-Ray XRAD 225Cx of which the absolute stage positioning was verified using an ultra sound sensor. Dose painting can be achieved by using simultaneous table and gantry movement during irradiation and would enable the delivery of complex heterogeneous dose distributions. The feasibility of this technique was investigated through the use of control point based treatment plans consisting of high numbers of control points. The need for non-coplanar irradiations was evaluated using cone-beam CT scans of tumor bearing mice, glioblastoma multiforme (GBM), at the right side of the brain. The tumor, healthy brain and other important structures such as the parotid and submandibular gland were delineated to evaluate treatment plans in which different degrees of freedom were utilized.

Results: SmART-Plan was successfully extended with modules for performing large number of dose calculations and performing beam-on time optimization. The XRAD 225Cx proved to be able to deliver treatment plans with beams consisting of several hundred control points, to mimic dose painting. Stage positioning during treatment delivery was very accurate and reproducible to well within 100 micrometer. A more detailed quantification of these data will be performed. Preliminary results from different GBM treatment plans indicate that non-coplanar irradiation does not considerably improve treatment plan quality in comparison with coplanar beam configurations.

Conclusion: To maximize the benefits of the capabilities of image-guided small animal radiotherapy platforms, treatment planning automation and inversion is required to deliver complex dose distributions. Since treatment goals and restrictions are different from the clinical setting, preliminary data indicates that non-coplanar irradiation does not provide considerable benefits over coplanar-only beam configurations for preclinical radiotherapy GBM treatments.

The impact of neoadjuvant therapy on the tumour microenvironment in colorectal cancer

T Boterberg (1), J Tommelein (1), L Verset (2), F Gremonprez (3), E Melsens (3), B Descamps (4), C Vanhove (4), P Demetter (2), M Bracke (1), O De Wever (1)

(1) Laboratory of Experimental Cancer Research (LECR), Department of Radiation Oncology and Experimental Cancer Research, Ghent University, Ghent, Belgium, (2) Department of Pathology, Erasme University Hospital, Université Libre de Bruxelles, Brussels, Belgium, (3) Department of Surgery, Ghent University Hospital, Ghent, Belgium, (4) Department of Electronics and Information Systems, Ghent University, Ghent, Belgium

Introduction: Pre-operative radio(chemo)therapy is used as a standard treatment before surgery to increase the chances of local control and the life expectancy of rectal cancer patients. However, when recurrence develops in the previously irradiated area, patients usually have a poor prognosis and they frequently suffer from serious morbidity due to local invasion of bone and nerves. A better knowledge of the mechanisms by which radiotherapy works and how its efficacy could be improved, could therefore be of great clinical importance. Tumors are nowadays considered as ecosystems, not only consisting of cancer cells, but also of several other apparently normal cells such as cancer-associated fibroblasts (CAF's), immune cells and endothelial cells. This project aims to study the effect of irradiation and more specifically of irradiated CAF's on colorectal cancer (CRC) cells.

Materials & Methods: Cultures of colorectal CAF's were irradiated with clinically relevant daily doses of 1.8 Gy for 10 days up to a dose of 18 Gy on a linear accelerator for clinical use. Subsequently, the CAF's secretome was extracted for further analysis and to be used to treat CRC cells in vitro. In an in vivo experiment, following intra-caecal injection of CRC cells (human luciferase-containing HT29-hCG-luc cells) in nude mice, the caecum was highly conformally irradiated to a dose of 10 Gy with the Small Animal Radiation Research Platform. These mice were treated weekly with R1507 (a monoclonal antibody against the Insulin-like Growth Factor-1 receptor (IGF-1R)) or saline as control. Finally, for clinical correlation of the results, tissue samples from previously irradiated rectal cancer patients were stained for α-SMA (used as a CAF marker) and phospho-mTOR (which is downstream the IGF-1R/AKT survival pathway).

Results: Treatment in vitro of CRC cells with the secretome of irradiated CAF's increased cell spreading, cell number, lactate release and glucose uptake. In addition, mRNA sequencing revealed differential gene expression between irradiated and non-irradiated CAF's. A protein array demonstrated a significantly increased secretion of IGF-1, which is known as a pro-survival factor, by irradiated CAFs, as compared to non-irradiated CAF's. The secretome of these irradiated CAFs was found to stimulate the IGF-1R/AKT survival pathway in CRC cells. The specificity of this stimulation could be demonstrated by the use of IGF-1R inhibitors. In the in vivo experiment 50% of saline treated and locally irradiated tumour-bearing mice showed haematogenous spread, whereas only 7% of R1507 treated and locally irradiated tumour-bearing mice developed haematogenous metastases. On the tissue samples from previously irradiated patients, CAFs were more numerous and this was accompanied by an increase in phospho-mTOR in CRC cells. The effect on patient outcome is currently under investigation.

Conclusion: These results demonstrate a bystander-type phenomenon in which IGF-1 release by irradiated CAF's alters the phenotype of adjacent CRC cells, promoting CRC progression through the IGF-1R/AKT survival pathway. RT protocols combined with IGF-1/IGF-1R targeting agents may improve rectal cancer treatment.

Role of osteopontin in glioblastoma radioresistance

A Henry (1), A Blomme (1), P Peixoto (1), N Goffart (2), F Lallemand (3), N Leroi (3), O Peulen (1), P Martinive (4), Y Habraken (5), A Turtoi (1), B Rogister (2), V Castronovo (1), A Bellahcène (1)

(1) Metastasis Research Laboratory, GIGA Cancer, University of Liège, Liège, Belgium, (2) GIGA Neurosciences, University of Liège, Liège, Belgium, (3) Laboratory of Biology of Tumor and development, GIGA Cancer, University of Liège, Liège, Belgium, (4) Department of Radiology, University Hospital Liège, Liège, Belgium, (5) Laboratory of Virology and Immunology, GIGA Cancer, University of Liège, Liège, Belgium

Introduction: Glioblastoma (GBM) is the most aggressive and common solid human brain tumor. Because of GBM heterogeneity, location and aggressiveness, none of the available treatment is curative. These treatments include maximal surgical resection, radiotherapy and concomitant or adjuvant chemotherapy with Temozolomide. However, the prognosis of adult patients with GBM remains poor and the survival outcome after treatment does not exceed 15 months. GBM-composing cells have developed many strategies to counteract these current therapies. Among the wide hallmarks acquired to survive, high osteopontin (OPN) expression correlates with lower overall and disease-free/relapse-free survival in all tumors combined, as well in brain cancer.

Our recent study (Lamour V and Henry A, IJC 2015) has demonstrated the role of OPN in the tumorigenicity of glioblastoma cells and its importance in the maintenance of the stem characters. In the continuation of this work, our recent studies focused on the potential role of OPN in the resistance of GBM cells to radiotherapy and its potential implication in the initiation of Double Strand Breaks (DSBs) repair mechanisms.

Aims: In the context of this study, different GBM cell lines (U251-MG, U87-MG and U87 Viii) were used to assess the role of OPN in the initiation of the DSBs repair mechanism after an exposure to gamma-irradiation.

Methods and results: We performed the transient transfection of different GBM cell lines (U251-MG, U87-MG and U87-MG overexpressing EGFR VIII) with siRNAs specifically directed against OPN. After irradiation, all these OPN-depleted cells consistently showed a lower induction of γ–H2AX compared to control (irrelevant siRNA) as evidenced by western blot and immunofluorescence techniques. Thereafter, clonogenic assays allowed to prove that the survival of OPN-depleted cells was affected after an exposure to irradiation. To assess the importance of OPN expression in the response to radiotherapy, an heterotopic xenograft model was used. In brief, IPTG-inducible U87 shOPN clones were injected subcutaneously in NOD-SCID mice and were allowed to form a tumor. When average tumor volume reached a predetermined size range, mice were treated (or not) with IPTG by intraperitoneal injection during five days. At the end of the treatment, tumors were selectively exposed to gamma-irradiation by using a small animal irradiator X-RAD 225Cx (Precision X-Ray Inc., North Branford, CT). One week later, mice were sacrificed and tumors were measured. In this pilot study, we observed that mice in which the tumor was depleted in OPN displayed a slight regression in the tumor growth compared to mice that received radiotherapy alone (no IPTG), where the tumor volume remained constant.

Conclusions: Taken together, these preliminary data meet the fact that OPN is important in the response of GBM to radiotherapy. The in vitro results converge to the fact that OPN might be implicated in the initiation of the DSBs repair following irradiation. Currently, we would like to investigate this hypothesis in vivo but also to check the effect of OPN depletion combined to radiotherapy on the survival of mice in an orthotopic xenograft model.

In vivo detection of invasive Head and Neck Squamous Cell Carcinoma by an anti-CD44v6 antibody

J Odenthal (1,2), M Rijpkema (3), D Bos (3), O Boerman (3), R Takes (1), P Friedl (2)

(1) Radboud University Medical Center, Department of Otorhinolaryngology and Head and Neck surgery, Nijmegen, NL, (2) Radboud Institute for Molecular Life Sciences, Department of Cell Biology, Nijmegen, NL, (3) Radboud University Medical Center, Department of Nuclear Medicine, Nijmegen, NL

Introduction: Molecular detection of tumor lesions using targeted near-infrared (NIR) conjugated antibodies represents a promising strategy to improve the surgical removal of invasive tumors while sparing adjacent tumor-free tissue. We compared potential molecular targets of Head and Neck Squamous Cell Carcinoma (HNSCC) and identify CD44v6 as suitable marker for in vivo detection of HNSCC in an invasively growing ortothopic HNSCC mouse model.

Materials & Methods: A systematic search of literature was performed to identify molecular markers in HNSCC with emphasis on detection of the invasion zone. Balb/c nu/nu mice carrying tumors of human HNSCC cells in the floor of the mouth received an anti-CD44v6 antibody (bivatuzumab) dual-labeled with (111)In-DTPA and IRDye800CW, or a dual-labeled isoytpic control antibody. Mice were monitored by SPECT/CT and fluorescence imaging followed by ex vivo biodistribution studies, histology and NIR microscopy.

Results: Based on expression in human HNSCC lesions, c-Met, CD44, CD44v6 and EGFR showed potential as markers for HNSCC imaging, with most consistent and high expression of CD44v6 in nearly all HNSCC tumors. SPECT/CT and fluorescence imaging showed effective tumor targeting of bivatuzumab with good concordance between both approaches. Biodistribution studies confirmed high and specific accumulation of the CD44v6-targeting antibody in the tumors with an average of 54 ± 11 % injected dose per gram compared to 5 ± 2 % injected dose per gram of the isotype control. Histology showed consistent probe distribution along tumor cell surfaces in the center and invasive tumor regions.

Conclusion: The study establishes CD44v6 as epitope for the detection of HNSCC to support NIR-guided surgery. The targeting of invasive cells indicates that intraoperative detection of high-risk CD44v6 expressing tumors might be feasible with this approach.

Establishment of a relevant mouse orthotopic lung cancer model for testing alternative treatment strategies combined with image guided radiotherapy

V Sosa Iglesias, S van Hoof, J Theys, L Schijns, A Groot, A Yaromina, N Lieuwes, L Dubois, F, Verhaegen, M Vooijs

Department of Radiotherapy (MAASTRO)/GROW – School for Developmental Biology & Oncology, Maastricht University, Maastricht, the Netherlands

Introduction: Lung cancer is the leading cause of cancer death worldwide. Despite current research advances in the field, alternative treatment strategies are needed to eradicate non-responsive and resistant tumors. In order to test these strategies, clinically relevant tumor models are essential. Therefore we have established an orthotopic non-small cell lung cancer (NSCLC) mouse model in which a single localized tumor nodule is formed and can be monitored using cone beam computed tomography (microCBCT) imaging using a small animal micro-irradiator (SmART). Our immediate aim is to correlate microCBCT imaging with a more sensitive technique: Bioluminescence (BLI), to detect the tumor as early as possible and to evaluate the feasibility of delivering an individualized radiation treatment (using a commercially available software: SmART-Plan) accurately to the moving lung of a mouse. Our ultimate goal is to evaluate new treatment strategies in a pertinent NSCLC model for human in mice.

Materials & Methods: Immunocompromised mice received an intrapulmonary injection in the top right lung with several different NSCLC cell lines. A 10 ul cell suspension of $1x10^6$ cells in a mixture of 80% matrigel and 20% contrast agent was injected. We have tested different depths and locations within the right lung. Tumor growth was monitored on average 1-2x/week using: microCBCT and BLI.

Currently we are evaluating the appropriate time point (based on tumor burden) to perform dose-response curves for irradiation treatment by delivering a single irradiation dose (maximum to the tumor and minimum to organs at risk), with a millimetric precision using several beams.

Results: The H1299 NSCLC cell line developed reproducibly a single localized tumor nodule in the site of injection. The other two cell lines tested (H460 and A549-luciferase) revealed to be highly metastatic and experiments with them were not pursued. The tumor cell lines were intrapulmonary injected between the 7^{th} and the 8^{th} rib at a depth of 6 mm. MicroCBCT imaging revealed to be suitable for tumor monitoring using an energy of 80 Kvp (0.4 Gy/scan). Using these settings we monitored the increase in tumor volume as a function of time. BLI imaging at different wavelengths will be acquired for the H1299-luciferase cell line in order to obtain information on the depth and size of the tumor. Quantification and correlation between microCBCT and BLI, recently integrated in the same micro-irradiator, are ongoing.

In addition to tumor growth monitoring, data on the implementation of a small animal irradiation treatment planning software (SmART-Plan) will be presented. We have monitored the breathing rhythm of mice under deep anesthesia and it follows a clear interval of a short inhalation phase followed by a 4 second resting phase; data that we intend to use in order to deliver an individualized irradiation plan with optimal planned tumor volume (PTV) margins.

Conclusion: Using the SmART-Plan and irradiation systems in orthotopic NSCLC models is a novel preclinical platform to evaluate novel treatments for NSCLC when combined with radiation, mimicking clinical practice for NSCLC patients.

High-precision proton irradiation to study dose volume effects in rat tissues

P van Luijk, RP Coppes

Departments of Radiation Oncology and Cell Biology, University Medical Center Groningen, University of Groningen, The Netherlands

Introduction: Aiming to reduce normal tissue effects associated with radiotherapy, many technological developments attempt to reduce dose to normal tissues. However, optimal use of such technologies requires knowledge of mechanisms underlying normal tissue damage and their relation to irradiated volume. Therefore, normal tissue effects were studied using highly accurate proton irradiation to different regions and volumes in the rat spinal cord, parotid gland, heart and lung.

Methods: Irradiation was performed using collimated high-energy protons. Collimator design was based on X-ray imaging (spinal cord), MRI (parotid gland) or CT scans (heart, lung) of age, sex and weight matched rats. Depending on the organ and irradiated sub-volume this typically resulted in 2-4% uncertainty in irradiated volume of that organ. Specifically, for partial irradiation of the spinal cord an in-line X-ray imager was used to yield a positioning accuracy of 0.1 mm. Finally, non-uniform irradiations were facilitated by sequential use of different collimators. Hind leg paralysis, breathing frequency changes and salivary flow rate and tissue histo-pathology were used to assess organ response.

Results: Spinal cord: Next to volume effects, low doses surrounding small volumes with a high dose effects were found to strongly impact the tolerance dose. In addition, large differences in tolerance dose were observed between differently shaped dose distributions that irradiate the same amount of spinal cord tissue. Taken together these observations indicate that irradiated volume is not good predictor of toxicity. The data, however, could be described accurately with a model in which tissue repair originating from non-irradiated tissue is possible over a limited distance into the irradiated tissue. Taken together these results suggest that regeneration plays an important role in the response of the spinal cord.

Parotid gland: Using a series of non-uniform irradiations we demonstrated that the response of the parotid gland critically depends on dose to its stem cells, mainly located in its major ducts. The importance of this anatomical location was confirmed in a retrospective analysis of clinical data. A prospective clinical trial to validate this finding is in progress.

Lung: Volume dependent mechanisms of lung toxicities were observed, where high volumes with low dose limiting early vascular/inflammatory responses inducing pulmonary hypertension and consequential cardiac problems, whereas low volumes displayed high or even no dose limiting late fibrotic response. Moreover, inclusion of the heart in the irradiation field strongly enhanced early lung responses.

Conclusion: Using high-precision proton irradiation of rat organs, we elucidated several mechanisms and critical targets for normal tissue damage. In general we found that, rather than dose to the organ, the development of toxicity strongly related to dose to functional sub-structures within the organ or even in other organs.

In general, in more parallel organized tissues it seems that a high dose to a small volume is better that a low dose to a large volume. Maintaining or enhancing the regenerating potential of the normal tissue seems warranted to further optimize radiation therapy.

Tumorigenic effects of irradiated and non-irradiated cancer-associated fibroblasts co-transplanted with tumor cells in vivo

M Tunset Grinde[1], J Vik[2], L Gorchs[2*], K A Camilio[3], S Al-Saad[1, 3], I Martinez-Zubiaurre[2], T Hellevik[4*]

[1] Dept. Radiology, University Hospital of Northern Norway; [2]Department of Clinical Medicine, University of Tromsø, [3]Department of Medical Biology, University of Tromsø, Norway and [4]Dept. Radiation Oncology, University Hospital of Northern Norway

Background: Cancer-associated fibroblasts (CAFs) are a heterogeneous group of cells found in large numbers inside and around solid tumors. In many cancer types, high abundance of intra-tumoral CAFs is associated with poor prognosis, and their role as important determinants of tumor establishment and progression is widely acknowledged. In the context of radiotherapy (RT), tumor responses to RT are greatly influenced by the microenvironment, especially considering that all tumor-associated host cells receive the same prescribed radiation dose as malignant cells. Given the fundamental role played by CAFs on general tumor growth regulation, we hypothesize that CAFs may change their phenotype and pro-malignant nature upon irradiation, and that this circumstance could influence the ultimate fate of tumors post-therapy. In this work we have been exploring a) whether irradiation alters the pro-malignant influence of CAFs in vivo; b) if different dose/fraction regimens exert different CAF-mediated tumor growth regulation; and c) the potential mechanism(s) behind the radiation-induced effects.

Methods: Human lung CAFs established in monolayer cultures were exposed to single dose (1x18 Gy) or fractionated (3x 6Gy) ionizing radiation prior to subcutaneous implantation in Balb-c nu/nu athymic mice, along with equal numbers of lung tumor cells (A549). Tumor growth kinetics was monitored over time. Tumor biological parameters including vessel density (CD31), tumor cell proliferation (Ki67), ECM deposition (Masson's Trichrome) and inflammatory reactions (macrophages/neutrophils) were analyzed on tissue specimens and digitally quantified.

Results: As expected, tumors resulting from co-implantation of tumor cells and CAFs grew faster than tumors generated with tumor cells alone; the first ones displaying double-size 40 days post-implantation. Interestingly, tumors grown in the presence of both single-high dose (1x18Gy) and fractionated (3x6Gy) irradiated CAFs displayed similar growth curves as the control group without CAFs, suggesting that CAFs lose their pro-tumorigenic effects after irradiation. Quantitative histopathology revealed that average microvessel density was 3-fold enhanced in tumors with irradiated CAFs. On the other hand, the desmoplastic reaction observed in tumors with CAFs was lost in tumors with irradiated CAFs. Neither proliferation nor inflammatory activity was changed between the four experimental groups.

Conclusions: The present results indicate that CAFs lose their pro-malignant phenotype after both single high-dose and oligo fractionated radiation exposure. A decrease in the intra-tumoral deposition of extracellular matrix could play a major role in the observed effects. Of note, an increase in microvessel density was perceived in tumors established with irradiated CAFs, but this reaction was not associated with increased tumor growth. Further studies on tumors externally irradiated by image-guided radiotherapy are needed to elucidate the importance of irradiated CAFs on tumor fate post RT treatment.

First preclinical studies in vivo evaluating therapeutic efficacy of radiation dose-painting: from conventional dose painting to “inverse dose painting”

A Yaromina(1), D Trani(1), M Granzier(1), W van Elmpt(1), R Biemans(1), N Lieuwes(1), AD Windhorst(2), L Dubois(1), F Verhaegen(1), P Lambin(1)

(1) Dept. of Radiation Oncology (MAASTRO), GROW, MUMC+, Maastricht, the Netherlands; (2) Department of Radiology and Nuclear Medicine, VU University Medical Center, Amsterdam, the Netherlands

Several years ago, preclinical studies have been initiated in our department to develop an in vivo model and protocol to test dose-painting (DP) strategies, that is the prescription of a non-uniform radiation dose distribution to the gross tumor volume (GTV), based on the image-guided identification of potentially radioresistant biological target volumes (BTVs). Feasibility as well as dosimetric accuracy for positron emission (PET) based DP using state-of-the-art clinical PET/CT (computed tomography) imaging and radiotherapy (RT) platforms has been demonstrated in a rat tumor model [1]. The irradiation workflow included the same steps applied in the state-of-the art high precision RT in patients, i.e. treatment planning by means of a clinical treatment plaining system, precise positioning using cone beam CT, VMAT irradiation including portal dosimetry.

As a next step, therapeutic efficacy of DP strategies based on 18F-fluorodeoxyglucose (FDG uptake) has been tested in rat rhabdomyosarcoma model [2]. In this study FDG was selected as a target for radiation dose boosting because many clinical studies had demonstrated that high pre-treatment FDG uptake associated with worse outcome and that tumor relapse after irradiation occurred preferentially in tumor areas with high FDG uptake. Two DP strategies were tested: 1) targeted dose escalation and 2) dose redistribution. In this study it has been also investigated whether tumor response is determined by the highest dose in BTV or the lowest dose in GTV. It was found that, while dose escalation to high FDG uptake was not superior to the same dose increase in low FDG uptake subvolumes, dose redistribution was even detrimental. This data are consistent with the hypothesis that tumor response is dependent on the minimum intratumoral dose.

Hypoxia is another promising target for dose escalation. However, 2-3 times higher radiation dose is required to overcome hypoxia-mediated radioresistance in tumors, which is clinically difficult to achieve. Therefore, to overcome this challenge, a novel combination treatment approach is being tested: 1) targeting hypoxic tumor cells with a hypoxia-activated prodrug TH302 and 2) at the same time inverse radiation dose-painting to boost tumor subvolumes with no/low drug uptake. The results of this pilot study suggest that the proposed strategy is as effective as a uniform dose escalation to the entire tumor volume but with a greater capacity to spare normal tissues.

References:

1. Trani D, Reniers B, Persoon L, Podesta M, Nalbantov G, Leijenaar RT, Granzier M, Yaromina A, Dubois L, Verhaegen F, Lambin P. What Level of Accuracy Is Achievable for Preclinical Dose Painting Studies on a Clinical Irradiation Platform? Radiat Res 2015, 183:501-10.

2. Trani D*, Yaromina A*, Dubois LJ, Granzier M, Peeters SG, Biemans R, Nalbantov G, Lieuwes NG, Reniers BR, Troost EG, Verhaegen F, Lambin P. Preclinical assessment of efficacy of radiation dose painting based on intratumoral FDG-PET uptake. Clin Cancer Res 2015 (in press).

Comparison of CBCT imaging, dose calculation and biological response for high z nanoparticles

KT Butterworth (1), M Ghita (1), SJ McMahon (1), S Osman (2), CK McGarry (1,2), S Roux (3), O Tillement (3), AR Hounsell (1,2) KM Prise (1)

Affiliations: (1) Centre for Cancer Research & Cell Biology, Queen's University Belfast, UK (2) Northern Ireland Cancer Centre, Belfast City Hospital, UK (3) Laboratory of Physical Chemistry and Luminescent Materials, University of Lyon, France

Introduction: High atomic number (Z) nanoparticles have a diverse range of potential applications in biomedicine and offer significant opportunity for theranostic strategies by combining enhanced imaging and therapeutic capabilities. Building on the our in vitro evidence supporting gold nanoparticles as radiosensitizers, we are applying the small animal radiotherapy research platform (SARRP, Xstrahl Life Sciences) to a range of in vivo studies aiming to demonstrate combined therapeutic efficacy and enhanced CBCT imaging for different high Z material nanoparticles.

Materials & Methods: Experiments were designed to assess enhancement of CBCT, tumor responses and dose calculations in animals bearing sub-cutaneous tumors established from the PC-3 human prostate cancer cells. Gold (AuDTDTPA) Gold-Gadolinium (AuDTDTPA-Gd) and gadolinium (AGuIX) nanoparticles were administered by intra-tumoural or intra-venous injection. CBCT output from in-phantom studies was compared to data obtained for different nanoparticle types and routes of administration at different energies and time points after injection.

Results: We present our findings using different nanoparticle platforms as contrast agents and radiosensitizers. Differential CBCT enhancement and tumour growth delay was observed for each of the particles and used a basis for optimisation of route of delivery and imaging parameters. Imaging and treatment planning studies highlighted a number of current challenges for accurate dose calculation using high Z nanoparticles in small animal models.

Conclusion: The use of nanoparticle agents for CBCT enhancement and radiosensitisation has much potential significant effort to determine the optimum parameters in preclinical model systems which accurately mimic clinical scenarios is needed for future translation to early phase trials.

Treatment Planning Solutions for the Small Animal Radiation Research Platform (SARRP)

N Cho (1), JW Wong (2), P Kazanzides (1)

Affiliations: (1) Department of Computer Science, Johns Hopkins University, Baltimore, Maryland 21218, USA (2) Department of Radiation Oncology and Molecular Radiation Sciences, School of Medicine, Johns Hopkins University, Baltimore, Maryland 21231, USA

Introduction: The Small Animal Radiation Research Platform (SARRP) delivers radiation via a set of fixed size collimators or a motorized variable collimator (MVC). Treatment Planning is provided by plugin modules for a customized 3D Slicer application. Dose computation is performed on a Graphical Processing Unit (GPU) using the superposition-convolution method, allowing computation for multiple beams in less than a minute. This enables inverse planning methods for complex dose volumes, such as a spherical dose shell and more generally for arbitrary solid and hollow shapes.

Materials & Methods: We first construct a spherical dose shell by intersecting multiple hollow cylinders, where each cylinder is created by moving the collimated beam in a circular pattern. The planning system begins with a number of uniformly distributed cylinders and computes the dose for each cylinder. The cylinder weights are optimized using a non-negative least squares method, where the objective is to achieve a target dose. For computational efficiency, we sample a large number of points on the sphere, rather than using all points. We did not include constraints for critical organs, but this could be handled by the least squares solver or by a linear programming method.

We are extending the above method to arbitrary shapes, where the cylinders must be replaced by shapes formed by extruding the target outline along each beam axis. To efficiently create solid shapes with the MVC, we developed an algorithm that decomposes it into a minimum number of rectangles of variable size. This is achieved by segmentation, simplification, and decomposition steps. The segmentation step creates a label map using the existing 3D Slicer tools. Then, the simplification step approximates the label map by a rectilinear polygon, the outer isothetic cover (OIC), which is the smallest polygon that fully encompasses the target area. The quality of the fit is determined by a user-selectable grid size. The next step is to decompose the polygon into the minimum number of disjoint sets of rectangles, using the Hopcroft-Karp algorithm. Dose computation is performed for each rectangle. The next step is to perform the optimization using a constrained least squares or linear programming method.

Results: A spherical shell with 5 mm radius and 1 mm thickness was generated starting with an initial configuration of 73 cylinders. The inverse planning algorithm required approximately 10 minutes on a laptop with Intel Core i7-4850HQ and NVIDIA GeForce GT 750M, for a CT volume of dimension 138 x 369 x 83. Most of this time was required for dose computation. 34 of the 73 cylinders were assigned positive beam weights, with the remaining 39 beams having zero weight. A histogram was created based on the 3,057 voxels in the central region (i.e., within 0.1 mm) of the shell. Mean dose was within 2% of the requested dose, with a standard deviation of about 13%. Future work includes changing weights within each cylinder, which corresponds to changing the circular velocity, rather than assigning a single weight to each cylinder. We have applied the rectangle decomposition algorithm to a single 2D shape, and our current work is to complete the optimization for MVC delivery of an arbitrary 3D solid shape.

Conclusion: The GPU-accelerated dose computation method for SARRP enables the implementation of efficient inverse planning methods for complex dose shapes, such as hollow and solid shapes. Preliminary results are demonstrated for delivery of a uniform spherical dose shell in heterogeneous tissue, as well as for decomposition of an arbitrary 2D cross-section into the minimum number of rectangles for delivery by a motorized variable collimator.

Frameless stereotactic radiotherapy alone and combined with temozolomide in canine gliomas

M Dolera, L Malfassi, S Pavesi, S Marcarini, M Sala, G Mazza, N Carrara, G Urso

La Cittadina Fondazione Studi e Ricerche Veterinarie, Romanengo - CR, ITALY

Introduction: Brain gliomas are diagnosed in an increased number of dogs. Few data regarding the best treatment regimen are available. The primary aim of this work was to evaluate the feasibility and efficacy of high dose hypo fractionated volume modulated arc radiotherapy (VMAT RT) in canine gliomas. The secondary aim was to assess the efficacy and toxicity of combination of radiotherapy with temozolomide.

Materials & Methods: 72 client owned dogs with imaging based or histologically confirmed diagnosis of brain gliomas were enrolled. LINAC based frameless stereotactic radiotherapy was offered to all dogs. Dogs whose owners refused RT were palliatively treated (palliation arm). The schedule of treatment has ranged between 33 Gy/5 fx and 42 Gy/10 fx according the volumetric dose constraints of the brain (RT arm). During the second phase of the study, the same RT treatment was offered combined with temozolomide (TMZ) 65 mg/m^2 orally administered 6 hours prior each fraction and then for 5 days monthly for 6 cycles (RT+TMZ arm). Regular clinical examinations were performed during and after irradiation time, with regard to mentation, deambulation, cranial nerve dysfunction and seizures. Serial magnetic resonance imaging exams were planned 2, 4, 6, 12, 18, 24 months after irradiation. Volumetric disease response and imaging findings were implemented with clinical neurological systematic evaluation to assess the course of the disease. Multivariate analysis to assess any prognostic significance was performed. Overall and disease specific survival were estimated using the Kaplan Meier curves.

Results: 30 dogs were palliated, 22 dogs were treated with RT, 20 were treated with RT+TMZ. Among RT arm, 7 dogs were treated with 42 Gy/10 fx, 15 dogs with 35 Gy/5 fx. Among the RT+TMZ arm, 10 dogs were treated with 42 Gy/10 fx, 2 dogs with 38 Gy/5 fx, 4 dogs with 35 Gy/5 fx, 4 dogs with 33 Gy/5 fx. 1 grade II radiotoxicity was observed. Median overall survival in palliated, RT and RT+TMZ arm was 94 days, 383 days, 420 days. 11/42 dogs have died from the brain tumor, 8/11 due to recurrent disease within the irradiation field, 3 due to spinal seeding. No statistically significant difference in survival was evident for the different grade of tumors (GII-GIII p=0.10; GIII-GIV p=0.68), presence of oedema, mass effect and between RT and RT+TMZ (p=0.61), whereas RT and RT+TMX were different from palliated (p=0.00089; p=0.000061). The significant prognostic factors were the relative volume of the tumor <5% (p=0.013) and the clinical presentation with no alteration mental status (p=0.032).

Conclusions: VMAT RT is feasible and effective for canine brain gliomas. Small tumors and normal mental status are positive prognostic factors. The combination with TMZ at the used dose don’t elicited any additional improvement in survival rate. Dose escalation in TMZ combination could be evaluated in further research.

Nanobody-Based Theranostics in Cancer

M D'Huyvetter

In Vivo Cellular and Molecular Imaging (ICMI) lab, Vrije Universiteit Brussel, Brussels, Belgium

Introduction: Targeted radionuclide therapy (TRNT) aims to specifically deliver cytotoxic radiation to tumor cells, with minimal uptake in healthy tissues. This is acchieved by targeting a unique or overexpressed antigen on tumor cells. So far the succes of TRNT using monoclonal antibodies (mAbs) as targeting vehicles has been limited, often due to unfavorable biodistribution and inadequate dose estimations. An emerging strategy to overcome these issues is called "theranostics". This principle integrates a preliminary imaging component to detect the presence and accessibility of a target, and will therefore allow the prediction of successful TRNT. To do so, we investigated the use of Nanobodies (nbs) as theranostic agents to image the presence of a tumor-specific target, and then to specifically deliver cytotoxic radiation to cancer cells. Nbs consist of the antigen binding subparts of heavy chain-only Abs, and are about 15 kDa in size. They show superior specificity, improved tissue penetration and fast off-target clearance.

Materials & Methods: The potential of radiolabeled nbs was evaluated in two relevant preclinical cancer models of (1) human epidermal growth factor receptor 2 overexpressing (HER2+) breast cancer and (2) multiple myeloma (MM). In a first part we describe the development and optimization of diagnostic and therapeutic radiolabeled anti-HER2 nbs against HER2, by means of biodistribution and efficacy studies. In a second part a similar strategy was applied on radiolabeled nbs that target MM cells.

Results: The lead compound anti-HER2 nb was successfully radiolabeled with diagnostic isotopes ^{99m}Tc, ^{68}Ga and ^{18}F for SPECT and PET imaging of HER2. For TRNT purposes, nb was radiolabeled with ^{177}Lu. After injection of ^{177}Lu-anti-HER2 nb, dosimetry estimations in xenografted mice revealed a dose of 0.90 Gy/MBq to both tumor and kidneys and extremely low doses to healthy tissues. In a parallel study we were able to reduce kidney retention of radiolabeled nbs to a minimum by adjusting the linker and/or the used radioisotope. Compared to ^{177}Lu-anti-HER2 nb, ^{177}Lu-Herceptin (anti-HER2 mAb) not only irradiated the tumor but also lung, liver, spleen, bone and blood. Nb-based TRNT in mice bearing small subcutaneous HER2+ tumors led to an almost complete inhibition of tumor growth. At the end of the study, a significant difference in overall survival was observed between treated and the control groups.
In addition, the potential use of nbs for imaging disease progression and TRNT of MM was investigated. Nbs were generated against the paraprotein (i.e. anti-idiotypic), produced by 5T2 MM cells. A lead nb was selected, after evaluating its capacity to target MM cells, via flow cytometry and SPECT imaging of MM mice. A prophylactic treatment in MM mice showed that ^{177}Lu-anti-idiotypic nb could inhibit disease progression by targeting the residual MM cells in bone marrow.

Conclusion: We were able to show that radiolabeled nbs are capable of targeting and eradicating tumor cells with high specificity, thereby halting tumor progression. Unwanted radiation to normal organs was low, suggesting a good safety profile. We therefore believe that radiolabeled nbs could act as a promising theranostic tool in cancer therapy.

A Comparison of 3-D Bioluminescence Radiation Targeting using Analytical and Monte Carlo Models of Light Propagation

RA Weersink (1,2), S Ansell (1), J Cassidy (3), V Betz (3), L Lilge (4), K Wang (1), DR Jaffray (1,2)

(1) Radiation Medicine Program, Princess Margaret Hospital, 610 University Ave, Toronto Canada,
(2) Techna Institute, University Health Network
(3) Department of Electrical and Computer Engineering, University of Toronto, Toronto Canada
(4) Department of Medical Biophysics, University of Toronto

Introduction: We have developed a system that integrates optical imaging with an existing image-guided small animal irradiator. The optical imaging enables bioluminescence imaging and imaging of x-ray excited-optically emitting agents, providing both high resolution anatomical imaging using cone beam CT and functional imaging using optical techniques. A primary purpose of this integration is to improve targeting of small tumors that are difficult to see on CBCT due to its limited soft tissue contrast but may be visible using bioluminescence. Our goal is to provide 3D targeting of the tumor based on BLI which requires fast methods of BLI reconstruction to determine the target location.

Materials & Methods: We have developed two methods of BLI source reconstruction. The first method is based on an analytical model of light propagation in tissue and assumes that the mouse consists of homogeneous tissue. The reconstruction consists solely of determining the center of mass of the bioluminescence source. While this method is fast, it is prone to error in anatomical locations where there are large differences in the optical properties of neighbouring tissues within the mouse. The second method uses Monte Carlo calculations of light propagation and can use either a homogeneous mouse or employ accurate tissue optical properties for each organ. This method requires deformable registration between the segmented mouse model and the CBCT of the sample mouse. An inverse solution is further required to determine the true size of the bioluminescent source. While more accurate, the time required for this calculation may be impractical for targeting radiation delivery in a timely manner.

Results & Conclusions: We will quantitatively compare the accuracy of the analytical model versus the Monte Carlo reconstruction. Errors in source position will be measured at typical anatomical sites including brain, lung, liver, and lower torso. The impact of tumor size will also be systematically investigated. The errors between the analytical and Monte Carlo models will be used to create margins for the planning target volume in the radiation delivery. The impact on targeting of radiation treatments using BLI will be discussed.

Optimizing dual energy CBCT protocols for preclinical imaging and radiation research

LEJR Schyns (1), PV Granton (1), IP Almeida (1), SJ van Hoof (1), B Descamps (2), C Vanhove (2), G Landry (3), F Verhaegen (1)

(1) Department of Radiation Oncology (MAASTRO), GROW – School for Oncology and Developmental Biology, Maastricht University Medical Centre, Maastricht, the Netherlands, (2) iMinds Medical IT - IBiTech - MEDISIP - INFINITY, De Pintelaan 185, 9000 Gent, (3) Department of Medical Physics, Ludwig-Maximilians-University, Munich 85748, Germany

Introduction: Dual energy CT (DECT) imaging is now commonly used for a wide range of radiological purposes, such as deriving virtual non-contrast images and improving metal artifact reduction techniques. However, for preclinical imaging and small animal radiotherapy purposes, DECT imaging is still unexplored. For DECT imaging, two images are acquired using scanning protocols with two different tube voltages and/or filters i.e. two different x-ray spectra. These images can be decomposed into effective atomic number (Z_{eff}) images and relative electron density (ρ_e) images. In external photon and proton beam radiotherapy, taking both Z_{eff} and ρ_e into account has been shown to increase the accuracy of dose calculations. In addition, DECT imaging can improve tumor visibility and (automatic) tissue segmentation, as different tissue types have different elemental compositions. The aim of this work is to investigate if DECT imaging is feasible for small animal irradiators with an integrated cone beam CT (CBCT) system.

Materials & Methods: Several measurements are performed using two in-house developed mini phantoms (30 mm diameter) with each 12 cylindrical inserts (3.5 mm diameter). One phantom, containing parts of tissue-equivalent inserts of a Gammex RMI 467 phantom, is used for calibration. The other phantom, containing parts of CIRS 002ED inserts plus other materials with known elemental compositions and electron densities, is used for validation. The mini phantoms are imaged using both an X-RAD 225Cx system and a Small Animal Radiation Research Platform (SARRP) for a series of tube voltages from 40 to 100 kVp in 10 kV increments for equal imaging doses. Separate calibrations are performed for each combination of tube voltages and Z_{eff} and ρ_e for each validation insert are derived for these tube voltages using the corresponding calibration set. The experimental DECT imaging is compared to simulations that are obtained using the ImaSim software package, which is also used to simulate different noise levels and beam hardening in different phantom sizes.

Results: The derived Z_{eff} and ρ_e for each validation insert are compared for the X-RAD 225Cx system and the SARRP. Both systems show the largest Z_{eff} and ρ_e discrepancies and standard deviations for DECT images that are acquired using similar tube voltages, because of the poorly separated x-ray spectra (spectral overlap). The optimal combination of tube voltages is found for well-separated spectra and depends on the noise level/tube current and the imaged object's size.

Conclusion: DECT imaging i.e. deriving Z_{eff} and ρ_e using small animal irradiators with an integrated CBCT system is feasible. Optimizing scanning protocols for the specific imaging goal is recommended.

Feasibility study of repetitive diffusion MRI after Neoadjuvant radiotherapy for following tumor microenvironment

F Lallemand [1,2,3], N Leroi[2], M Bahri[3], EBalteau[3], A Noël[2], P Coucke[1], A Plenevaux[3], P Martinive [1,2]

1 Department of Radiotherapy-Oncology, CHU de Liège, ULg, Belgium
2 Laboratory of Tumor and Development Biology, ULg, Belgium
3 Cyclotron Research Centre, University of Liège, Liège, Belgium

Purpose/Objective: Neoadjuvant radiotherapy (NeoRT) improves tumor local control and tumor resection in many cancers. The timing between the end of the NeoRT and surgery is mostly driven by the occurrence of side effects or the tumor downsizing. We previously demonstrated in an in vivo model that the timing of surgery and the schedule of NeoRT influenced the tumor dissemination. Here, our aim is to evaluate with functional MRI (fMRI) the impact of the radiation treatment on the tumor microenvironment and subsequently to identify non-invasive markers helping to determine the best timing to perform surgery for avoiding tumor spreading. First, we needed to demonstrate the feasibility of repetitive MRI imaging after NeoRT in mice.

Materials & Methods: We used two models of NeoRT we previously developed in mice: MDA-MB 231 and 4T1 cells implanted in the flank of mice. When tumors reached the planned volume, they are irradiated with 2x5 Gy and then surgically removed at different time points after RT. In the mean time between the end of RT and the surgical procedure, mice were imaged in a 9,4T Agilent® MRI. Diffusion Weighted (DW) -MRI was performed every 2 days between RT and surgery. For each tumors we acquired 8 slices of 1 mm thickness and 0.5 mm gap with an “in plane voxel resolution” of 0.5 mm. For DW-MRI, we performed FSEMS (Fast Spin Echo MultiSlice) sequences, with 9 different B-values (from 40 to 1000) and B0, in the 3 main directions. We also performed IVIM (IntraVoxel Incoherent Motion) analysis, in the aim to obtain information on intravascular diffusion, related to perfusion (F: perfusion factor) and subsequently tumor vessels perfusion.

Results: As preliminary results, with the MBA-MB 231 we observed a significant increase of F at day 6 after irradiation than a decrease and stabilization until surgery. No other modifications of the MRI signal, ADC, D or D* were observed. We observed similar results with 4T1 cells, F increased at day 3 than returned to initial signal. The difference in the timing of the peak of F can be related to the difference in tumor growth between MBA-MB 231 and 4T1 (four weeks vs one week).

Conclusion: For the first time, we demonstrate the feasibility of repetitive fMRI imaging in mice models after NeoRT. With these models, we show a significant peak of the perfusion factor (F) at day 6 or day 3. This change occurs between the two previous time points of surgery demonstrating a difference in the metastatic spreading. Indeed, after a NeoRT of 2X5Gy we observed more metastases in the lung when MDA-MB 231 tumor bearing mice are operated 4 days after RT compared to 11 days. These preliminary results are very promising for identifying noninvasive markers for determining the best timing for surgery.

MRT (Microbeam Radiation Therapy (MRT): achievements and future perspectives

E Bräuer-Krisch[1]
on behalf of the MRT scientific MRT collaborations

[1] ESRF, European Synchrotron Radiation Facility, Grenoble, France

Abstract: Microbeam Radiation Therapy (MRT) is a novel technique[1] using spatially fractionated, intense, highly collimated, parallel arrays of X-ray beams generated at 3rd generation synchrotron facilities like the ESRF in Grenoble, France. The insertion of an adequate multislit collimator[2] produces microbeams with a FWHM between 20 and 100 µm with separations between 100 and 400 µm to be delivered at an extremely high dose rate (up to 20kGy/sec) to best exploit the dose volume effect with peak entrance dose values well above several hundreds of Gy, demonstrating a very high normal tissue tolerance even for the immature tissue [3]. The differential effects[4] between normal tissue vasculature and tumor vascular networks promote this novel approach and questions one of the dogmas in radiation therapy: namely, that radiation therapy is aiming at a dose distributions with the primary goal to maximize the dose at the target, while minimizing the dose to the normal tissue in order to generally optimize the treatment in cancer therapy. An overview of the most important findings in radiation biology as well as achievements in Medical Physics will be summarized reflecting the current status of the project.

Keywords: Microbeams, Synchrotron, MRT, Radiation Therapy.

Bedside to Bench in Normal Tissue Radiobiology: translating patient experience into animal models

B Koontz

Duke Cancer Institute Durham NC USA

Introduction: Normal tissue radiobiology has developed hand in hand with advents in treatment paradigms. Initial fractionation studies exploited differences in tumor and normal tissue response to radiation. Recent advances in stereotactic radiotherapy exploit technology to minimize in field normal tissue, but tolerances and tissue response to high dose per fraction must be respected.

Materials & Methods: Using clinical examples of the toxicity related to treatment for prostate and other cancers, we developed stereotactic animal models to explore normal tissue radiobiology and explore potential radioprotective agents.

Results: Small animal irradiation can be used to mimic human radiotherapy by providing accurate and homogenous dose to focal target organs. Focal irradiation of prostate can provide insight into origin of rectal, bladder, and sexual injury. Our data supports injury of both microvascular and micro-innervation causing organ dysfunction. Experiment using focal irradiation can be used to test potential strategies for radioprotection in support of clinical protocol development.

Conclusion: Using clinical principles of common toxicities, animal models of focal irradiation can be used to investigate the molecular response to radiation in normal tissues and to develop interventions for future clinical use.

Radiation-induced lung damage promotes breast cancer lung-metastasis: use of SARRP in an orthotopic mouse model of breast cancer

L Feys[1], B Descamps[2], C Vanhove[2], A Vral[3], L Veldeman[4], S Vermeulen[5], C De Wagter[4], M Bracke[1], O De Wever[1]

[1]Department of Radiation Oncology and Experimental Cancer Research, Laboratory of Experimental Cancer Research, Ghent University, Ghent, Belgium

[2]Department of Electronics and Information System, iMinds-IBiTech-MEDISIP, Ghent University, Ghent, Belgium

[3]Department of Basic Medical Sciences, Physiology Group, Ghent University, Ghent, Belgium

[4]Department of Radiation Oncology and Experimental Cancer Research, Gent University Hospital, Ghent, Belgium

[5]Department of Biomedical Science, HoGent, Ghent, Belgium

Introduction: Radiotherapy is a mainstay in the postoperative treatment of breast cancer as it reduces the risks of local recurrence and mortality after both conservative surgery and mastectomy. Despite recent efforts to decrease irradiation volumes through accelerated partial irradiation techniques, late cardiac and pulmonary toxicity still occurs after breast irradiation. The importance of this pulmonary injury towards lung metastasis is unclear.

Materials & Methods: Syngeneic orthotopic breast cancer mouse models were used to irradiate partial volumes of lung by SARRP, metastasis formation was monitored through bioluminescence imaging. Cell cultures models were used for investigating the associated molecular mechanisms.

Results: Preirradiation of lung epithelial cells induces DNA damage, p53 activation and a secretome enriched in the chemokines SDF-1/CXCL12 and MIF. Irradiated lung epithelial cells stimulate adhesion, spreading, growth, and (transendothelial) migration of human MDA-MB-231 and murine 4T1 breast cancer cells. These metastasis-associated cellular activities were largely mimicked by recombinant CXCL12 and MIF. Moreover, an allosteric inhibitor of the CXCR4 receptor prevented the metastasis-associated cellular activities stimulated by the secretome of irradiated lung epithelial cells. Furthermore, partial (10%) irradiation of the right lung significantly stimulated breast cancer lung-specific metastasis in the syngeneic, orthotopic 4T1 breast cancer model.

Conclusion: Our results warrant further investigation of the potential pro-metastatic effects of radiation (Feys et al., Oncotarget;6:26615-32, 2015).

Transforming mice into mini-humans: A valid strategy for translational research?

D De Ruysscher (1, 2), L Dubois (1), M Vooijs (1), P Lambin (1), F Verhaegen (1)

(1) Dept Radiation Oncology (Maastro), GROW - School for Oncology and Developmental Biology, Maastricht University Medical Centre, Maastricht, The Netherlands
(2) Radiation Oncology, KU Leuven, Leuven, Belgium

Clinical research faces many problems, of which the availability of pre-clinical models that predict the human situation is one of the most important. Pre-clinical tumour models are being used for decades, assuming that they are predictive for what will later happen in humans. Indeed, the use of pre-clinical, mostly mouse, models may limit the exposure of inactive and or toxic treatments in patients. Although there is no doubt that pre-clinical models have been crucial to understand better molecular and other characteristics of carcinogenesis, growth and metastases and were the basis of many currently used cancer therapies, they still have considerable shortcomings. Classical mouse models use tumour cell lines that have been grown in vitro for many years and hence may have altered characteristics compared to de novo tumours. These tumour cells are then implanted subcutaneously in mice and tend to grow rapidly and thus do not mimic the much slower doubling times of most human cancers. This faster tumour growth may lead to a higher sensitivity for most chemotherapy drugs and hence erroneous conclusions. Moreover, in some situations, ectopic (out of the normal place) subcutaneously implanted tumours — still a standard methodology — may respond differently to treatment compared to tumours grown in an orthotopic site, i.e. in their organ or tissue of origin, such as breast cancers in mammary fat pads. The latter may correspond more to the human situation. Moreover, metastases frequently show other responses than primary tumours in patients, and it is only recently that these effects can be mimicked in genetically engineered mouse models. Tumour bearing mice are often treated with drugs at levels, or with pharmacokinetics, that are not relevant to humans. Furthermore, nearly all pre-clinical models have not used tumours that were pre-exposed to another therapy, whereas in many phase I and phase II clinical trials only patients that show tumour progression after one or more systemic treatments are included. More specifically for radiotherapy research, most pre-clinical series deal with single-fraction irradiation of subcutaneous tumours without any imaging. In normal tissue research, generally very large volumes are treated with radiation dose distribution that are by no means representative for the real clinical world. Typically, only small volumes of organs at risk (OAR) receive high doses, whereas large volumes get low doses. The strong dose-volume dependency of radiation effects thus makes most pre-clinical radiation dose-volume relations quite unreliable.

In recent years, pre-clinical models have improved significantly. The genetic background of mouse strains is better defined and environmental factors such as diet or the microbiome have been incorporated. Computational modelling for gene-gene and gene-environmental interactions have been developed together with genome engineering and improved phenotyping. Patient-derived orthotopic xenografts mimic responses to chemotherapy and targeted agents in specific conditions and fully immunocompetent tumour models have increased our knowledge on the tumour-host-immune interaction.

However, an ideal mouse model does not exist. All models have drawbacks and never reflect the full range of complexity of the tumour and the host of patients. Many promising agents in pre-clinical research fail in human studies and possibly some therapeutics that fail in a pre-clinical model may have been beneficial for patients. The most realistic attitude may therefore be to select features that are appropriate for a certain research question in patients, investigate which mouse model (tumour or normal tissue) display similar features as the ones in humans, and perform pre-clinical studies in these models.

Spatial frequency dosimetric performance limitations for dose optimization in preclinical investigations

JMP Stewart (1,2), PE Lindsay (2,3), DA Jaffray (1-4)

(1) Institute of Biomaterials and Biomedical Engineering, University of Toronto (2) Radiation Medicine Program, Princess Margaret Cancer Centre (3) Department of Radiation Oncology, University of Toronto (4) Department of Medical Biophysics, University of Toronto (5) The Techna Institute for the Advancement of Technology for Health, Toronto

Introduction: Modern image-guided microirradiators have provided the foundation for technically challenging preclinical and radiobiological investigations. Such systems are typically able to deliver radiation fields down to a size of approximately 1 mm with sub-millimeter targeting accuracy and beam falloff on the order of a millimeter. These capabilities have raised interest in optimizing and delivering heterogeneous dose distributions for preclinical investigations such as bath-and-shower normal tissue experiments, vascular targeting strategies, and functional imaging derived dose prescriptions. Recent progress in preclinical inverse dose optimization strategies has begun to address this need, but these techniques are fundamentally limited by the dose delivery `optics' of fixed radiation field geometries and finite beam penumbras. In this work, we quantify this limit and show that it is an optimization-independent function of the mutual spatial frequency content of the desired dose distribution and the collimated radiation field delivered by the microirradiator.

Materials & Methods: The dosimetric performance limitation was developed under the assumption that the delivered dose is a superposition of one or more fixed radiation beam kernels (delivered, for example, with a single collimated field in a step and shoot fashion). In this framework, a lower bound on the difference between an arbitrary desired dose distribution and an optimized dose distribution was derived as the sum of spatial frequencies in the desired dose distribution which had a larger magnitude than the spatial frequencies of the fixed dose kernels. The utility of the bound was quantified through two two-dimensional dosimetric challenges: a 'bullseye' distribution consisting of five 1 mm wide circular rings alternating between 0 and 2 Gy, and a 'sock' composite dose distribution with a 1 Gy 1.5 mm exponentially decaying region, a 1 Gy homogeneous 1.5 x 4 mm region, a 7.5 x 4 mm region with a linear dose increase from 0 to 1 Gy over 7.5 mm, and a 2 mm radius semicircle with constant 1 Gy dose. For each desired dose distribution, an optimized dose distribution was calculated for delivery with a 1 mm circular collimator with a previously developed step-and-shoot algorithm and the results compared to that derived from the analytic performance bound.

Results: The derived performance limitation determined a lower dosimetric bound of 23.6% and 14.4% across the dose distribution for the bullseye and sock distributions, respectively, as measured as a proportion of the total desired dose. The optimization algorithm yielded dose distributions with a corresponding dosimetric difference of 33.6% and 25.1%

Conclusion: The spatial frequency dosimetric performance limitation rigorously quantifies the difficulty of optimizing and delivering spatially varying dose distributions and informs the design and evaluation of optimization and radiation field targeting methods.

The impact of breathing motion on a mouse lung tumor irradiation using the 4D MOBY phantom

B van der Heyden, S van Hoof, L Schyns, F Verhaegen

Maastro CLINIC

Introduction: A mouse is breathing during precision irradiation of a tumor. If a tumor is located in the lung, this tumor can move along with the diaphragm. During the irradiation there is a possibility that the tumor partially moves out of the small fields used in precision irradiation. The tumor motion cannot be seen on the CT scan and the irradiation device does not have a 4D CT mode to record the tumor displacement as a function of time. There is a possibility to do fluoroscopic imaging, but this method provides insufficient information to perform dose calculations.

Materials & Methods: The mathematical 4D MOBY phantom with a 4mm lung tumor is used to simulate a breathing mouse. Respiratory motion of an anesthetized mouse is simulated in different time frames using a realistic breathing function. The MOBY anterior-posterior and diaphragm parameters of this function are determined by analyzing fluoroscopic images of a mouse under anesthesia. Each static frame is loaded in SmARTPlan and is treated by a full arc radiation with a 5mm circular collimator. Because all the dose calculations are done on static frames, the dose values have to be rescaled to the averaged organ treatment dose for the tumor, lungs, spinal cord and heart. The tumor location is simulated at different heights in both left and right lung. The mean rescaled organ doses are compared in eight different cases (four in each lung).

Results: If the tumor is located near the diaphragm, the relative difference between the expected (without motion) and the calculated mean dose (with motion) is -11%. This difference decreases when the tumor is positioned higher in the lung. If the tumor is located in the upper part of the lung this relative difference is within the range of -1%. The relative difference in heart dose strongly depends on the lung tumor position and thus the irradiation field. It depends less on the location in the left or right lung. In each of the eight cases the mean spinal cord dose remains constant.

Conclusion: The impact of breathing motion on the tumor dose strongly depends on the tumor position. If the tumor is located near the diaphragm the relative difference between the expected and the calculated mean doses becomes larger. Due to breathing there is an overestimation of the tumor dose, the difference is large enough to take into account in the treatment plan. The results will also depend on the breathing motion pattern, which could depend e.g. on species and anesthesia.

Intra- and inter- fraction variation in animal position for multi-fraction lung radiation on a small animal radiation research platform

CL Eccles (1), J Thompson (1), L Bird (1), MA Hill (1), WG McKenna (1), KA Vallis (1)

(1) CRUK/MRC Oxford Institute for Radiation Oncology, University of Oxford

Introduction: The development of image guided small animal irradiators facilitate pre-clinical radiotherapy (RT) experiments that simulate the clinical situation, i.e., the use of online image guidance, conformal or small field irradiation, and multi-fraction RT. With the availability of online image guidance, the reproducibility of radiation delivery can be verified, just as it is done clinically, using portal imaging or cone beam ct. This work presents inter- and intra- fraction reproducibility of CBA mice undergoing 3-fraction radiation to the right lung using parallel opposing fields on an Xstrahl small animal radiation research platform (SARRP) system.

Materials & Methods: Twenty-six 10-12 week old CBA mice underwent image-guided radiation to the right lung using a custom collimator and parallel opposed pair technique on alternate days for three fractions. Following anaesthetic induction, sedation was maintained using continuous isoflurane (2%). Animals were imaged and irradiated vertically in a custom made Perspex holder, with the gantry at 90^{O} to the vertical. The holder incorporated a compressible balloon to monitor breathing rate, a heating pad and a rectal temperature probe. The holder included 1 mm polycarbonate windows on the front and back over the RT region to minimize X-ray attenuation within the treated volume. The main body of the collimator was constructed from brass with additional lead with an open aperture to define the irradiation field incident on the mouse enabling one lung to be irradiated while minimising dose to the other. Imaging was performed using 50 kVp X-rays, while RT exposures were performed using 220 kVp x-rays using the collimator to define the irradiation field. To check alignment, single planar X-ray images were acquired with and without the collimator and the resulting images overlaid to identify the RT field with respect to the mouse anatomy. Following RT from one side, the mouse was rotated through 180^{O} and the alignment was confirmed again. Using the superior and lateral aspects of the rib-cage, and superior and lateral field edges, intra- and inter- fraction changes in animal position were determined.

Results: 156 portal images of the 12 mm x 6 mm radiation fields were assessed and the absolute random (σ) and systematic (Σ) intra-fraction errors were 0.20 mm and 0.10 mm in the right-left (R-L) direction and 0.44 mm and 0.22 mm in the caudal-cranial (C-C) direction respectively. Inter fraction errors were larger with Σ= 0.29 mm in the R-L and 0.34 mm in the C-C directions; random errors were 0.25 mm and 0.45 mm in the R-L and C-C directions. The mean procedure time was 20 minutes (range 11 – 31 mins) and the greatest intra-fraction variations (i.e., ≥ 0.3mm) occurred on fractions that required ≥ 17 minutes for the delivery of both beams.

Conclusion: To our knowledge this is the first intra- and inter- fraction image guidance reproducibility study in a pre-clinical model. The results confirm image guidance is useful for assuring animal positioning reproducibility between fractions, and that minimal positional changes occur over the course of a single fraction.

Development of a novel analytical dose calculation software for small animal radiotherapy

M Reinhart (1), M Fast (1), S Bartzsch (1), S Nill (1), U Oelfke (1)

(1) Joint Department of Physics at The Institute of Cancer Research and The Royal Marsden NHS Foundation Trust, London, UK SM2 5NG

Introduction: High precision irradiators for small animals offer the possibility of mimicking state-of-the-art patient treatments and are expected to advance the understanding of dose-effect relationships and radiobiology in general. We aim to implement IMRT-like treatment methods for small animal radiotherapy, focusing on the development of a treatment planning system capable of inverse planning. The first step towards such a planning tool is to develop an underlying dose engine, which has to permit fast dose calculations. The use of kV photons introduces additional challenges compared to patient treatment due to the increased importance of the photoelectric effect and the resulting material dependence. We present a kernel based dose calculation engine for kV irradiations of small animals.

Materials & Methods: The backbone of the dose engine is an analytical point kernel algorithm originally developed by Bartzsch et al. (Med Phys 40, 111714 (2013)) for micro-beam radiotherapy. The central idea is that interactions of keV photons and electrons with matter can be treated separately, due to their different ranges in tissue. For small animal radiotherapy, the range of electrons and the voxel size are of the same order of magnitude. Therefore, we do not consider electron transport explicitly but assume local energy deposition. The photon interactions are separated into the energy transferred at the primary interaction point, and all subsequent scattered events. The primary dose is calculated analytically, and all further energy deposition is treated in a point kernel approach.

We translated the algorithm outlined above into a C++ program, capable of forward-calculating the dose based on a CT image and the treatment parameters. The developed dose engine was validated against Geant4 Monte Carlo (MC) simulations for various phantoms and beam configurations. The dose distributions were evaluated in water, and slab phantoms of water with 1cm thick bone, lung and muscle tissue inserts at 2cm depth.

Results: Reasonable agreement was found for all cases. For field sizes of 5mm to 1cm in water, the depth dose curves agree within 2% (mean). The largest deviations are found in the entrance region (5%) and at large depths (6%). For slab phantom geometries including bone, lung, and muscle inserts, larger differences are observed at the material interfaces. While the absolute deviations in the depth dose can reach up to 15% for the bone slab, the overall agreement is within 3% (mean). For lung and muscle inserts, the depth dose curves agree within 9% at the tissue interfaces and 2% overall (mean).

Conclusion: The presented dose calculation algorithm yields promising results for the use in inverse treatment planning. Good agreement with MC simulations was observed in a set of initial studies. The deviations at tissue interfaces are an inherent issue of kernel-based approaches, while the discrepancies at larger depth can be attributed to the energy sampling. Further investigations will address both problems as well as the calculation time. The algorithm has the potential to become a sufficiently accurate but significantly faster alternative to full MC simulations.

Plastic scintillating optical fiber dosimetry for small animal irradiation

C Le Deroff (1), A-M Frelin Labalme (1,2), X Ledoux (1)

(1) Grand Accélérateur National d'Ions Lourds (GANIL), CEA/DSM-CNRS/IN2P3, Boulevard Henri Becquerel, 14076 Caen, France
(2) Archade, Centre François Baclesse, 3 Avenue du Général Harris, 14076 Caen, France Email address presenting

Small animal image-guided irradiation systems deliver millimetric beams of medium X-ray energy, scaled to small animal size. The dosimetry of such beams represents a major challenge since few adapted dosimeters exist yet. Plastic scintillating optical fiber dosimeters are promising candidates for this particular application since they combine small detection volume, direct reading and a composition close to that of water. They have been widely studied for high energy dosimetry and have been shown to be very well suited to mega- voltage beams. Nevertheless, their response is less known at lower energy particularly because of scintillation quenching. Therefore our work concerns the development and the characterization of such a dosimeter for small animal irradiation dosimetry. Particular care has been taken for energy dependence study in low and medium energy range.

Our dosimeter prototype, called Dosirat, is composed of a 1mm diameter and 15mm long plastic scintillating fiber (BCF-12, Saint Gobain) coupled to clear optical fiber. The light output signal induced by irradiation is measured by a photodiode coupled to an electrometer. All irradiations have been performed with the image-guided X-Rad 225Cx irradiator (PXI Inc.) installed in Caen in the frame of Archade project. Repeatability, reproducibility and linearity measurements have been performed to evaluate Dosirat performances in large field conditions (225kV, 13 mA, and 10cm x 10cm field size). Dosirat response to energy has then been evaluated for different tube voltages (20 to 225kV) and filtrations (2mm Al, 0.3mm Cu and none). The measurements have been compared to air kerma measurements performed with two calibrated ionization chamber (PTW23342 and PTW30013) and to energy deposition computations using Monte Carlo simulation (GATE and MCNP).

Our dosimeter has shown excellent repeatability (<0.1%), linearity (correlation coefficient > 0.99) and noise to signal ratio (<0.6%) in large irradiation field. It has been found that its sensitivity depends on energy and beam quality. The simulations have allowed to differentiate sensitivity variation due to mass energy- absorption coefficient variations from scintillation quenching. They have also shown the high dependence of energy deposition computations on the energy spectra below 50keV. Hence energy spectra measurements are needed to validate low energy simulations. Then beam energy spectrum modifications due to irradiation conditions and attenuation in different media (water, tissues...) will be simulated to investigate the impact of energy dependence for in vivo implementation. After the validation of the response of scintillating fiber dosimeters to kilo-voltage beams, a smaller probe will be tested in small irradiation fields.

These results show good dosimetric performances of scintillating fiber dosimeters at medium energy despite their energy dependence. Nevertheless an accurate knowledge of its response in function of the energy make it very suitable when used at a given beam quality. In consequence, scintillating fiber dosimeters remain promising tools for small animal dosimetry thanks to their small size, convenient composition and real-time readout capability.

Biologically optimized commissioning study for small animal irradiation platform

M Ghita (1), H Thompson (1), K Butterworth, CK McGarry (1,2), SJ McMahon (1), AR Hounsell (1,2) KM Prise (1)

(1) Centre for Cancer Research & Cell Biology, Queen's University Belfast, UK; (2) Radiotherapy Physics, Northern Ireland Cancer Centre, Belfast City Hospital, UK

Introduction: Pre-clinical studies have become increasingly more sophisticated in the radiation biology field, and with this the demand of more advanced radiation platforms for small animal studies. The paradigm is that the new generation of small animal radiation platforms are better able to mimic the technologies available in a modern radiotherapy clinic. The Small Animal Radiation Research Platform (SARRP) is a technological development which enables state-of-the-art image guided therapy (IGRT) research to be performed on small animal models. By combining high-resolution cone–beam computed tomography (CBCT) imaging with an isocentric irradiation system, the SARRP offers capabilities of mimicking modern clinical systems which integrate a linear accelerator and on-board X-ray guidance(Wong et al. 2008; Matinfar et al. 2009). Similar to any clinical Linac or accessory device, the SARRP and associated CBCT require rigorous routine quality assurance. The gap between radiotherapy clinic and the laboratory incldues the use of different radiation protocols and therefore the results obtained in a uniform radiation field are difficult to translate into a high-dose multiple beam arrangement. Building a protocol for quality assurance and treatment delivery procedures, while linking the outcome with biological results, is an important step in overcoming the differences between radiotherapy clinic and laboratory protocols. Biological cross-calibration with an existing broad beam irradiation source was used to assess the field uniformity in broad beam configuration. Furthermore, geometrical and dosimetry accuracy has been tested and further studies will interrogate the presence of other biological processes in the same configuration.

Materials & Methods: Initial commissioning assessed the doses in air and a solid water phantom and cross calibrated them with EBT3 films using optical density. The Depth Profiles and cross-beam profiles for each aperture were obtained using EBT3 gafchromic film following the X-Strahl commissioning specifications. Broad field dosimetry was biologically validated using colony survival and DNA damage assay in a panel of cell lines. Biological output has been cross calibrated with a PXI XRAD 225kVp uniform field irradiator. The treatment delivery of two parallel opposed beams and CBCT scanning were validated using a DNA damage assay.

Results: A good agreement between the measured depth doses and the data provided by Xstrahl for all apertures was found. Furthermore, in an open beam configuration, biology data confirms a field uniformity comparable to the one provided by a uniform field irradiator. The delivery of two parallel opposed beams will induce DNA damage comparable to that expected from a standard single field radiation.

Conclusion: A significant step in translating laboratory radiobiology into radiotherapy outputs is overcoming technological differences in the radiation modalities used for human treatment and pre-clinical research. The synergistic integration of radiotherapy physics and biology has the great potential to improve the outcome of future cancer treatment. The technical aspects such as Commissioning and Quality Control need to be aligned with those used in radiotherapy clinic and also with the standards currently used in radiation biology laboratories to improve the translational output of radiobiology experiments.

Matinfar, Mohammad, Santosh Iyer, Eric Ford, John Wong, and Peter Kazanzides. 2009. "IMAGE GUIDED COMPLEX DOSE DELIVERY FOR SMALL ANIMAL RADIOTHERAPY:" 1243–1246.

Wong, John, Elwood Armour, Peter Kazanzides, Iulian Iordachita, Erik Tryggestad, Hua Deng, Mohammad Matinfar, et al. 2008. "High-Resolution, Small Animal Radiation Research Platform with X-Ray Tomographic Guidance Capabilities." International Journal of Radiation Oncology, Biology, Physics 71 (5) (August 1): 1591–9.

A new ESTRO work group on recommendations for standardization for small animal radiation research

F Verhaegen, L Dubois, S Gianolini, M Hill, C Karger, D Sarrut, D Thorwarth, C Vanhove, B Vojnovic, J Wilkens, R Weersink, K Lauber, K Prise, D Georg

Precision (Image-Guided) Small Animal RadioTherapy (SmART) is a novel field of pre-clinical research, where the aim is to investigate the action of radiation, possibly in synergy with other agents, in models for tumors and normal tissue in small animals. Both fundamental radiobiology and pre-clinical trials are the goal of this field. The novelty of the field is in the very precise radiation beams that are applied to the animal models, possibly guided by high-resolution imaging and sophisticated treatment planning. This new research field is enabled by the availability of novel equipment for precision irradiation and imaging.

The newly established ESTRO work group's mandate is to review the current state of the art in this new field, but also to review current practice in the field of radiation research with conventional radiation cabinets or linear accelerators. The work group will issue recommendation on how to use the available technology optimally to achieve best standard practice.

Abstracts
Posters

1. Characterization of PTW's "microDiamond" detector in small animal radiotherapy research x-ray beams

S Kampfer (1,2), JJ Wilkens (1,2)

(1) Department of Radiation Oncology, Klinikum rechts der Isar, Technische Universität München, Munich, Germany
(2) Physik-Department, Technische Universität München, Munich, Germany

Introduction: The Small Animal Radiation Research Platform (SARRP) from Xstrahl (Xstrahl Ltd., UK), a commercially available system with a 225 kV x-ray tube, is designed for very small field irradiations, e.g. in mice. One of the big challenges in quality assurance measurements for preclinical high precision radiotherapy is to find an appropriate measuring device for small fields. The recently presented single crystal diamond detector (SCDD) from PTW (PTW-Freiburg, Germany), called microDiamond (µD, type TM60019), could potentially be used in this environment.

Materials & Methods: We tested this µD detector (active volume: 0.004 mm^3, volume thickness in the detector axis: 1 µm) for its suitability to measure relevant properties of the beam. To measure the lateral profiles of the beam, the orientation of the detector was perpendicular to the beam axis. To characterize the influence of a rotation around its axis (roll), we measured the angular dependence of the µD detector in the used beam quality with on open field. The lateral profile measurements were then done in the isocenter in 2 cm depth and with a fixed roll. In order to perform a depth dose measurement we first checked the dose rate linearity of the detector in an open field by varying the tube current. During this and the following measurements the axis of the detector was parallel to the beam axis. The depth dose measurement itself was done with a fixed SSD of 304 mm. The beam profiles and depth dose curves were measured for two field sizes: 5x5 mm^2 and 10x10 mm^2 and compared to the results of film measurements with radiochromic films (Gafchromic EBT3, Ashland, USA). All measurements were done in solid water slabs or PMMA phantoms with a 220 kV beam with a current of 13 mA, except for the linearity measurement.

Results: Due to a distinct angular dependence of the detector, the rotation has to be kept within a range of about 50° to be used for perpendicular measurements. The lateral beam profiles resulted in 10.1 mm for the field width of the 10x10 mm^2 field, and in 5.1 mm for the 5x5 mm^2 field. In comparison to the measurements with the film (10.2 mm, and 5.2 mm respectively), this means a very good agreement (differences less than 0.1 mm or 1% for the bigger and 0.12 mm or 2.4% for the smaller field). No difference was seen for the dose rate linearity of the µD detector compared to our standard ionization chamber, which was also used to calibrate the µD for the depth dose measurement. The measured depth dose shows values of 3.71 Gy/min in 5 mm and 1.14 Gy/min in 51 mm. Film measurements produced 3.68 Gy/min in a depth of 5.3 mm and 1.16 Gy/min in 51.4 mm, which means also very good agreement of the two methods (maximum deviation of about 2%).

Conclusion: Our results imply the ability of the µD detector for quality assurance measurements in preclinical research x-ray beams, as long as the fields have dimensions of at least several millimeters.

2. Combination of external beam radiotherapy and molecular radiotherapy (^{131}I-MIBG) for the treatment of human neuroblastoma xenografts

A Corroyer-Dulmont(1), N Falzone(1), V Kersemans(1), J Thompson(1), D Allen(1), J Beech(1), S Gilchrist(1), P Kinchesh(1), S Able(1), B Vojnovic(1), I Tullis(1), S Smart(1), K Vallis(1)

Affiliations: (1) CRUK/MRC Oxford Institute for Radiation Oncology, Department of Oncology, University of Oxford, Old Road Campus Research Building, Off Roosevelt Drive, Oxford OX3 7LJ, United-Kingdom

Introduction: Neuroblastoma is the most frequent extra-cranial tumour in younger childhood. The current treatment of high-risk (stage 4) inoperable neuroblastoma includes a combination of chemotherapy and/or total irradiation with either autologous bone marrow transplantation or peripheral blood stem cell reinfusion. Despite these treatments the 4-year overall survival for high-stage neuroblastoma is still low (69%). Another approach involves targeted/molecular radiotherapy (MRT) where the overexpressed noradrenaline transporter is targeted with ^{131}I-MIBG (Meta-iodobenzylguanidine) an analogue of noradrenaline. The aim of this study is to investigate whether in vivo imaging could be used to optimize and measure EBRT enhanced efficacy of MRT with ^{131}I-MIBG in a human neuroblastoma xenograft model (SK-N-SH).

Materials & Methods: To assess the effect of combined EBRT and MRT, a SK-N-SH cancer xenograft model in nude mice was developed. Vessel permeability was evaluated with dynamic, contrast-enhanced MRI (DCE-MRI) to optimize scheduling of MRT (20 MBq) after an initial EBRT (5 Gy - SARRP irradiator) treatment. A subsequent EBRT dose (5 Gy) was delivered to simulate a fractionation scheme combining EBRT and MRT. Survival (as time needed to obtain a set limit tumour volume) was assessed and tumour volumes were determined at different times with MRI.

Results: DCE-MRI showed an increase in vessel permeability at 24h but not at 72h after EBRT treatment, and resulted in MRT being delivered 1 day after EBRT. Tumour growth was rapid in the control group and these animals were euthanized within 7 days. ^{131}I-MIBG caused a significant delay in the growth rate of the tumours in comparison to the control group ($p<0.01$) and the tumours were observed to shrink during the initial 5 days after dosing. However a recurrence was observed at day 7. More interestingly, EBRT treatment 1 day before or 1 week after MRT treatment significantly decreased the tumour volume (from 500mm^3 at day 0 to 40mm^3 at day 7; $p<0.001$ vs control and MRT alone group) and increased the overall survival.

Conclusion: This study demonstrated that the combination of EBRT and MRT potentiated the therapeutic effect in a neuroblastoma model and confirmed that MRI could be used to monitor this effect. Furthermore it emphasized the importance of scheduling the combined treatment according to pathophysiological criteria such as vessel permeability.

3. Metabolomic analyzes of the tumor microenvironment after neoadjuvant radiotherapy

N Leroi[1]; S Blacher[1]; F Lallemand[1,2,3]; J Leenders[4]; P De Tullio[4]; P Coucke[3]; A Noël[1] ; P Martinive[1,3]

[1] Laboratory of Tumor and Development Biology, Giga Cancer, ULg, Belgium
[2] Research center of Cyclotron, ULg, Belgium
[3] Department of Radiotherapy-Oncology, CHU de Liège, ULg, Belgium
[4] CIRM, Chimie Pharmaceutique, Ulg, Belgium

Purpose: Neoadjuvant radiotherapy (RT) is used in many case of cancer and aims at improving tumor local control and patient overall survival. RT schedule and the timing of surgery are mostly empirical based on clinical experiences, however in the case of Locally advanced rectal cancer, the timing of surgery following neoadjuvant RT appears crucial for patient overall survival (Coucke et al., 2006). Therefore, we hypothesized that radiotherapy may influence the tumor phenotype as well as the tumor microenvironment and consequently metastasis formation. We developed a pre-clinical model of neoadjuvant RT to study the impact of different RT schedules on TME and metastatic dissemination and tried to predict metastatic profile with metabolic profile of the tumor at the time of surgery.

Materials & Methods: We developed unprecedented in vivo model mimicking neoadjuvant RT used in clinic, we subcutaneously injected human mammary cells (MDA-MB-231) into the flank of SCID mice. Once tumors reached 400mm³, we locally irradiated the primary tumor with different neoadjuvant RT schedules (5x2Gy and 2x5Gy) inspired from clinical practice but adapted to mice. We surgically removed tumors 4 or 11 days after the end of RT and kept the mice alive during 6 weeks for metastatic growth. Then we sacrificed the mice and looked for lung metastases highlighted by human Ki-67 immunohistochemical staining. Tumor extracts were analyzed by Nuclear Magnetic Resonance (NMR).

Results: The occurrence of lung metastases is totally different according to the radiotherapy schedule and the time of surgery. After 2x5Gy, the size and the number of lung metastases were smaller when surgery was performed at 11 days after the end of RT, compared to 4 days. Inversely, in the 5x2Gy schedule, applying surgery at 4 days protected the mice against lung metastases compared to surgery at 11 days. Tumor volumes are the same in all groups and cannot be incriminated in the difference of lung metastases. Or aim here, is to determine predictive marker of the risk of tumor dissemination based on the tumor metabolism waste. Thanks to NMR analysis and powerful statistical tools, the study of the primary tumor at the time of surgery showed different metabolic profiles according to the RT schedule. Moreover, we were able to observe a correlation between this metabolic profile and metastatic profile for individuals in the different groups.

Conclusion: We developed a powerful in vivo model of neoadjuvant radiotherapy allowing us to demonstrate the impact of neoadjuvant RT schedule and the timing of surgery on metastatic profile. Moreover, NMR analyses and discriminant analyses showed an impact of neoadjuvant radiotherapy on tumor microenvironment that could be correlated to the metastatic profile.

4. Longitudinal study of lung fibrogenesis in Wt and RhoB deficient mice

B Petit(1), PG Montay-Gruel(1), G Boivin(1), MC Vozenin(1)

(1) Radiation Oncology Laboratory / Radiothérapy, CHUV, Lausanne, Switzerland

Despite technological breakthroughs, radiotherapy still induces acute and long term disabling side effects. The medical options available to prevent or treat them are scarce and developing effective countermeasures is still an open research field. Former studies suggested that rhoB expression was associated with normal tissue (Vozenin, 2004[1]) and tumour (Ader, 2003[2]) radiosensitivity. In this project we used a X-Rad 225Cx to locally irradiate wt and RhoB deficient C57Bl6 mice and investigated acute and delayed lung response by CT-scan imaging and histology. RhoB-/- and C57bl/6 mice were irradiated with small animal RX-irradiator (X-Rad 225Cx). Whole lung irradiation was performed using a 15mm circular collimator at 14 Gy. Local lung irradiation was performed using a 5mm collimator at 20Gy. Longitudinal imaging was performed by CBCT at various time points. Lungs were also collected at various time points for histological analyses. After localized 14Gy whole-lung irradiation, 50% RhoB-/- mice died within the first 12W versus 0% in the WT group. Histological analyses indicate RT-induced acute pneumonitis in RhoB-/- showing abnormal lymphocytes infiltration. Consistently, quantification of Hounsfield unit showed a transient enhancement 2 weeks post-RT, followed by a latency phase and a progressive re-induction during the fibrogenic period, more severe in RhoB deficient animals. These results identify RhoB as a novel radioprotective gene. RhoB radioprotective action seems to be mediated by preservation of hematopoietic and epithelial stem cells and control of acute inflammation that subsequently mediate beneficial acute wound healing process.

[1]-Vozenin-Brotons MC, Milliat F, Linard C et al. Gene expression profile in human late radiation enteritis obtained by high-density cDNA array hybridization. Radiat Res 2004; 161: 299-311.
[2]-Ader I, Delmas C, Bonnet J et al. Inhibition of Rho pathways induces radiosensitization and oxygenation in human glioblastoma xenografts. Oncogene 2003; 22: 8861-8869.

5. Optimization of planning for Liver irradiation using contrast enhancement and CBCT

B Petit(1), N Melin(2), PG Montay-Gruel(1), K Sprengers(1-3), LV Tran(1-3), B De Bari(1), E Herrmann(4), D Stroka(2), MC Vozenin(1)

(1) Radiation Oncology Laboratory / Radiotherapy, CHUV, Lausanne, Switzerland; (2) Visceral Surgery and Medevine, University of Bern, Bern, Switzerland; (3) Bachelor of Science Radiologic Medical Imaging Technology, University of Applied Sciences Western Switzerland, Lausanne, Switzerland; (4) Departement of Radiation Oncology, Bern University Hospital, and University of Bern, Switzerland

Technological developments have been made in radiation oncology and allow more precise target delineation and three-dimensional treatment planning for optimal delivery of radiation to tumor targets while sparing surrounding organs. However, in the liver radiation-induced liver disease (RILD) remains a problem and development of experimental models of RILD and hepatocarcinoma is needed both for mechanistic and therapeutic interventions. Therefore our objective was to optimize liver imaging in mice using X-Rad 225Cx-CB-CT. We aimed at enhancing liver contrast in order to improve liver delineation and irradiation using X-Rad 225Cx. For that purpose we used ExiTron nano 6000 (Miltenyi Biotec) as contrast agent and imaged healthy mice at various time point after injection (up to 40 days). Kinetics study show enhanced Hounsfield Unit level by 300 fold as soon as 1h post-injection and maximal enhancement of the contrast 8h post-injection. This study shows the feasibility of contrast enhancement to optimize liver imaging and contouring.

6. Investigation of Radiation and Vitamin D Effects on Asymmetric Arginine, Homocysteine on Rats

E Kahraman (1), A Arıcıoğlu (1), M Akmansu (2)

(1) Gazi University Health Sciences Institute, Department of Biochemistry, (2) Gazi University Medical Faculty, Department of Radiation Oncology, Ankara, Turkey

Introduction: Increased level of Asymmetric Dimethyl Arginine (ADMA) is associated with endothelial dysfunction. Additionally, irradiation has harmful effect on endothelial cells. Increased Homocysteine (Hcy) level is another factor leading to endothelial dysfunction. In this study, radiation induced oxidative stress and Vitamin D effects on endothelial injury are investigated through ADMA and Hcy levels.

Materials & Methods: 24 female wistar albino rats were divided into 4 groups of 6 rats. Groups were arranged as follows: Group 1: Control Group, Group 2: Irradiated Group, Group 3: Irradiation + Vitamin D Group, Group 4: Vitamin D Group. Group 3 and Group 4 rats were given Vitamin D for a week. In the end of the week, Group 2 and Group 3 rats received total body irradiation by SAD technique with 612cGy gamma rays. On the 8^{th} day, blood samples were taken from all rats, through which ADMA and Hcy levels are examined.

Results: In Group 2, Vitamin D levels decreased and Hcy levels increased. ADMA level in Group 2 slightly increased. In Group 3, Hcy levels decreased whereas ADMA levels increased. ADMA levels decreased only in Group 4.

Conclusion: In this study, it is observed that irradiation reduces Vitamin D level significantly. It is seen that Vitamin D supply helps to prevent radiation induced oxidative stress.

Key Words: Radiation, Vitamin D, Hcy, ADMA, oxidative stress

7. A designated web based database and evaluation tool for monitoring of small laboratory animal radiation experiments

Th Frenzel (1+2), C Grohmann (1), U Schumacher, A Krüll (2)

(1) Universitätsklinikum Hamburg-Eppendorf, Zentrum für Experimentelle Medizin, Institut für Anatomie und Experimentelle Morphologie, Martinistraße 52, 20246 Hamburg, Germany
(2) Universitätsklinikum Hamburg-Eppendorf, Ambulanzzentrum des UKE GmbH, Bereich Strahlentherapie, Martinistraße 52, 20246 Hamburg, Germany

Introduction: Small animal experiments are still required for basic cancer research. The regulatory requirements to conduct the experiments are becoming more and more stringent so that seamless monitoring and documentation of animals' health condition has an increasing importance. Precise documentation of all scientific results is mandatory as well. For this reason, we developed a designated web based database and evaluation tool for our experiments.

Materials & Methods: Our experiments have been performed with hundreds of laboratory animals. Radiotherapy [1], radio-chemotherapy, and chemotherapy groups were compared with control groups. Several researchers we working with the data at the same time. For this reason, standalone solutions we not possible and a designated web based database and evaluation tool was created to fulfilled all of our needs [2].

Results: Our web-based MySQL database consists of 54 single tables which are logically coupled. The graphical user interface was created using HTML (PHP for scripting) and CSS. Access to is possible through any kind of computer or handheld device that has an implemented web browser. Animal ward rounds (condition, weight, stress of the animals, etc.), type and numbers of tumor cells injected, tumor size, anesthesia, chemotherapy given (name of chemotherapeutic agent, concentration, volume applied, etc.), radiation dose applied (physical dose, time, fractionation, maximum dose allowed, etc.), supplemental nutrition, and much more data is stored. The tables can be queried with all kinds of SQL commands. Several reports were implemented, e.g. a "general report" for each animal describing all of its treatments, tumor size during radiotherapy, condition score, etc.

All information is stored in one database and not spread over several files on different computers, which makes it easier to evaluated the data. As data is stored in the web, access is possible at any place in the world with internet access which allows for international cooperation projects. As we implemented evaluation functions as well it is more than just a collection of data but also a tool to evaluate our experiments. E.g. multiple tumor growth curves for selected groups of animals can be exported into Microsoft Excel files which enables further processing of the data.

8. Radiotherapy and PD-1 blockade promote synergistic antineoplastic efficacy in Kras-mutant murine lung cancer

GS Herter-Sprie (1,2,3), S Koyama (1,2,4), H Korideck (5,7), J Hai (1,2,3), J Deng (1,2,3), CL Christensen (1,2,3), JM Herter (8), GM Makrigiorgos (5,7), GJ Freeman (1,2,4), G Dranoff (1,2,4), PS Hammerman (1,2,3), M Hallek (9,10), AC Kimmelman (6,7), KK Wong (1,2,3,11)

(1) Dept of Medicine, Harvard Medical School, Boston, (2) Dept of Medical Oncology, Dana-Farber Cancer Inst, Boston, (3) Lowe Center for Thoracic Oncology, (4) Cancer Vaccine Center, (5) Div of Medical Physics and Biophysics, (6) Div of Genomic Stability and DNA Repair, (7) Dept of Radiation Oncology, Dana-Farber Cancer Institute, Brigham and Women's Hospital, Harvard Medical School, Boston, (8) Center for Excellence in Vascular Biology, Dept of Pathology, Brigham and Women's Hospital, Harvard Medical School, Boston, USA, (9) Dept of Internal Medicine, Center of Integrated Oncology, University of Cologne, Germany, (10) Cologne Cluster of Excellence in Cellular Stress Responses in Aging-Associated Diseases (CECAD), Cologne, Germany, (11) Belfer institute for Applied Cancer Science, Dana-Farber Cancer Institute, Boston

Introduction: Radiation therapy (RT) is a critical nonsurgical treatment in the management of solid malignancies including lung cancer, but many patients experience local recurrence with or without metastatic disease. The cytoreductive effect of RT is well known, however, emerging evidence suggests that this antitumor therapy may provoke critical immune responses facilitating the therapeutic efficacy. Upon RT, tumor cells release various damage-associated molecular patterns (DAMP), which support the recruitment and activation of antigen-presenting cells and priming of tumor antigen-specific T cell responses. Regardless, immune-escape frequently arises resulting in disease progression, and thereby remains the leading cause of mortality in patients receiving RT. The identification and modulation of key immunmodulatory molecules within the tumor microenvironment is warranted to improve patient-tailored multimodal treatment options. Currently, we observe promising antitumor efficacy with the incorporation of agents targeting the PD-1/PD-L1 (programmed cell death protein 1) immune checkpoint.

Materials & Methods: Two distinct *Kras*-driven genetically engineered mouse models (GEMMs) of non-small cell lung cancer (NSCLC) were utilized in this study. Upon intrathoracic application of Cre, single nodule murine lung cancer driven by oncogenic $Kras^{G12D}$ (*K*) alone or in addition to deletion of the tumor suppressor gene *Stk11/Lkb1* (*KL*) was initiated. RT was given at a fractionation scheme of 8.5Gy x 2 on two consecutive days using the small animal radiation research platform (SARRP) at Dana-Farber Cancer Institute. PD-1 blocking antibodies (clone 29F.1A12) or vehicle (PBS) were given i.p. (200 µg/mouse) three times per week starting six hours after the second radiation dose. Tumor growth was evaluated every two weeks using MR imaging until the tumor burden met euthanasia criteria. Tumor and tumor-associated immune cells were identified and counted by flow cytometry analysis.

Results: We demonstrate that RT and PD-1 blockade promote major and durable antitumor efficacy in *Kras*-driven murine NSCLC. The combination treatment resulted in significant volume reduction of the target lesion, whereas single treatment with either RT or anti-PD-1 antibody only induced stable disease. While tumors of the latter regrew after 8-10 weeks on treatment, tumors of the combination therapy responded beyond 12-14 weeks. Timing of the anti-PD-1 application critically impacted on the therapeutic outcome. Concurrent treatment had synergistic efficacy in radiation naïve tumors; however, anti-PD-1 application in RT-resistant tumors had no antitumor effect and further induced T cell inhibitory markers in this setting. Furthermore, we observed that additional loss of the tumor suppressor *Stk11/Lkb1* rendered these lesions less responsive to the combinatorial therapy.

Conclusion: We provide evidence that clinical evaluation of combined RT and immunmodulatory therapy with anti-PD-1 appears promising for patients with *KRAS*-driven NSCLC. Given our observation that inhibition of the PD-1/PD-L1 axis in RT-resistant *K* tumors yields enhanced expression of T cell inhibitory markers on tumor-infiltrating T cells, we suggest dual checkpoint blockade as a potential treatment option in this setting. We found that molecular alteration of *Stk11/Lkb1* majorly impacted on the tumor-associated immune microenvironment and subsequently on the therapeutic response. Thus, alternative immunmodulatory concepts to optimally harness the therapeutic efficacy of RT and the adaptive immune response are required for this genotype.

9. Development of a small animal hyperthermia device

J Crezee (1), NAP Franken (1,2), A Bel (1), LJA Stalpers (1), CRN Rasch (1), HP Kok (1)

(1) Department of Radiation Oncology, (2) Laboratory of Experimental Oncology and Radiobiology, Academic Medical Center, University of Amsterdam

Introduction: Hyperthermia, induction of a temperature rise in the tumor of 41-43°C, is a vital component of multi-modality cancer treatments as it is a proven radio and chemosensitizer with excellent clinical results. Purpose of this work is to develop a small animal hyperthermia device, comparable to small animal radiotherapy devices. This small animal device should permit the same focused tumor heating as the systems that are used for clinical hyperthermia in humans.

Start of project: The design is a miniature version of the clinical AMC hyperthermia device for locoregional heating of deep seated tumors, consisting of a ring of tiny microwave antennas operating at 2.45 GHz positioned around the body of the mouse. The energy from the individual antennas can be focused onto almost any target volume within the body of the mouse. Researchers from five academic centers, AMC-University of Amsterdam, VUmc-Free University Amsterdam, Maastro–University of Maastricht and ErasmusMC, Rotterdam and the TU Delft compiled a program of seven research projects investigating various aspects of hyperthermia using this device. This project proposal was submitted to the Netherlands Organisation for Scientific Research NWO to finance construction of a small animal hyperthermia device.

Next steps: February 2016 an NWO medium investment grant was granted for this device. Construction will start under supervision of a user committee from the aforementioned institutes.
When the device becomes operational, the planned research projects will improve our knowledge on fundamental working mechanisms of hyperthermia. This will help to improve and optimize clinical protocols using hyperthermia in cancer treatments and reveal new promising research directions for the application of hyperthermia.